DESIGN AND FABRICATION OF ELECTRIC DUCTED

FAN FOR Unmanned Aerial Vehicles

_____

A Final Year Project Report

Presented to

SCHOOL OF MECHANICAL & MANUFACTURING ENGINEERING

Department of Mechanical Engineering

NUST

ISLAMABAD, PAKISTAN

_____

In Partial Fulfillment

of the Requirements for the Degree of

Bachelors of Mechanical Engineering

_____

by

Anees Hassan Khan

Syeda Saneeha Naqvi

Bilal Ahmed

Muhammad Abdullah Baig

June 2023

EXAMINATION COMMITTEE

We hereby recommend that the final year project report prepared under our supervision by:

NAME   REGISRATION NUMBER.

NAME   REGISRATION NUMBER.

NAME   REGISRATION NUMBER.

Titled: "Electric Ducted Fan for unmanned aerial vehicles" be accepted in partial fulfillment of the requirements for the award of Bachelors of Mechanical Engineering degree with grade ___

Supervisor: Dr. Emad ud Din Affiliation	 Dated:
Committee Member: Name, Title (faculty rank) Affiliation	 Dated:
Committee Member: Name, Title (faculty rank) Affiliation	 Dated:

_____   _____

(Head of Department)   (Date)

COUNTERSIGNED

Dated: _____   _____

(Dean / Principal)

i

ABSTRACT

This thesis demonstrates the designing and fabricating procedure of electric ducted fans (EDF) used in aerospace and other applications. The primary design parameters include the blade design, duct length, duct shape, duct diameter, and duct clearance. The blade design is critical in determining the thrust, power, and efficiency of the fan. The duct design parameters such as length, shape, diameter, and clearance have significant impacts on the aerodynamics and performance of the fan. It is crucial to optimize these parameters to achieve the desired balance between performance, efficiency, and structural integrity of the fan. Computational fluid dynamics (CFD) simulations and Finite Element Analysis (FEA) are useful tools for optimizing these design parameters.

ACKNOWLEDGMENTS

ORIGINALITY REPORT

TABLE OF CONTENTS

LIST OF TABLES

LIST OF FIGURES

ABBREVIATIONS

UAV	Unmanned Aerial Vehicle
EDF	Electric Ducted Fan
AOA	Angle of Attack
BET	Blade Element Theory
CFD	Computational Fluid Dynamics
RPM	Rotations Per Minute

NOMENCLATURE

D_p	Propeller diameter
K_p	Thermal losses of solar collector $((\text{W/m}^2)/°\text{C})$
r	Arbitrary distance from hub to blade element
J	Advanced ratio
AF	Activity Factor
Re	Reynolds Number
ρ	Air density
μ	Kinematic viscosity of air
v	Dynamic viscosity of air
V_∞	Cruise velocity/Forward speed of aerial vehicle
V_R	Resultant velocity
V_E	Effective velocity
w	Elemental induced velocity
Ω	Angular velocity of propeller
α	Elemental angle-of-attack
α_i	Induced AOA
β	Pitch angle
ϕ	Helix angle

c	Chord length
L	Lift Force
C_l	Coefficient of lift
D	Drag Force
C_d	Coefficient of drag
T	Thrust
Q	Torque
P	Power
ε_d	Diffuser expansion ratio
A_{exit}	Exit area of the duct
A_R	Rotor disc area
V_{exit}	Velocity of air at the exit of duct

CHAPTER 1: INTRODUCTION

Designing and manufacturing propellers and fans in the aeronautical industry of Pakistan is a novel and unique idea. It is a step towards innovation in technology and a requirement to boost our aeronautical industry. Designing and fabricating an electric ducted fan for a small Un-Manned Aerial Vehicle (UAV) promise to create a propulsion system that is efficient, safe, and practical for a wide range of applications, while also addressing the specific challenges of EDF design. An electric ducted fan (EDF) is a propulsion system used in small aircraft and drones that involves an electric motor powering a multi-bladed fan inside a duct, providing both lift and forward thrust.

Objective of the Project:

The objective of designing an electric ducted fan (EDF) allows a more efficient and powerful propulsion system for various applications, such as remote-controlled aircraft, drones, and electric-powered jets. Compared to traditional propellers, an EDF system operates by pulling air into an enclosed duct and then accelerating it through a fan, which produces a more efficient and streamlined airflow. The main advantages of an EDF system are higher thrust-to-weight ratios, increased efficiency, reduced noise levels, and improved safety due to the enclosed fan. Additionally, EDFs offer better control and maneuverability, which makes them ideal for certain applications such as indoor flying and acrobatics. Overall, the objective of designing an EDF is to create a reliable and efficient propulsion system that can be used in a wide range of applications.

Components of an EDF:

The conceptual design of an EDF involves several key components:

Motor:

> The motor is the heart of the EDF and is responsible for generating the power required to turn the fan. The motor should be selected based on the size and weight of the aircraft, as well as the desired speed and thrust.

Fan:

> The fan is a multi-bladed propeller housed inside a duct, which increases the system's efficiency by reducing turbulence and providing a more uniform airflow. The number of blades, blade shape, and size of the fan will depend on the specific requirements of the aircraft.

Duct:

> The duct is a tube-shaped structure that surrounds the fan and helps to direct the airflow. The duct should be designed to provide optimal thrust while minimizing drag and noise.

Battery:

>The battery is the power source for the motor and should be selected based on the required flight time and weight limitations

Application of EDF for Small UAV:

The project's main goal is to get the optimum performance for the particular aircraft or drone by balancing thrust, weight, and efficiency. There are numerous uses for designing an EDF for a small bird in the military, in agriculture, in monitoring, etc. It provides access to fresh and creative concepts that can be used in day-to-day life:

Surveillance and Reconnaissance:

>EDF-powered UAVs are advantageous for military, law enforcement, and border patrol applications because they can be fitted with cameras and other sensors to give real-time surveillance and reconnaissance data.

Agriculture:

>Small UAVs with EDFs can be used for crop monitoring and mapping, as well as for spraying pesticides and fertilizers.

Inspection and Maintenance:

>EDF-powered UAVs can be used for inspecting power lines, pipelines, and other critical infrastructure, as well as for maintenance and repair tasks in hard-to-reach locations.

Search and Rescue:

>EDF-powered UAVs can be equipped with thermal imaging cameras and other sensors to aid in search and rescue operations.

Aerial Photography and Videography:

>EDF-powered UAVs are commonly used for aerial photography and videography, especially in the film and entertainment industries.

Environmental Monitoring:

>Small UAVs with EDFs can be used for environmental monitoring, such as tracking wildlife populations, mapping forest fires, and monitoring air and water quality.

History of Ducted Fans:

A ducted fan is an airfoil-shaped propeller enclosed inside a cylindrical duct that resembles a wing. The duct around the propeller is necessary for the UAV's propulsion system since it produces more static thrust with the same size and power input. The UAV's overall acoustics are enhanced, and the duct also helps to reduce noise.

The Use of Material Innovation in the EDFS Design:

Electric ducted fans (EDFs) are designed with consideration for material innovation because it can have a substantial impact on the effectiveness and performance of these devices. Materials for electric ducted fans (EDFs) have been utilised since the beginning of electric motors and aircraft. The following are some of the main materials that have been employed over time:

1. Wood: Because it was readily accessible and simple to manufacture with, the original EDFs used wooden fan blades and frames. However, wooden fans were bulky and only performed so well.
2. Aluminium: Due to its light weight and ease of machining, aluminium became a common material for EDFs in the middle of the 20th century. Fan blades, motor housings, and other parts were made of aluminium.
3. Plastic: Nylon and ABS, two plastic materials that were more readily available in the 1970s, were utilised to make fan blades and other parts. Plastic fans were thin and simple to create in large quantities.
4. Carbon fibre: Due to its lightweight, high strength, and stiffness, carbon fibre quickly gained popularity as a material for high-performance EDFs in the 1990s. Fans constructed of carbon fibre could operate more efficiently and at faster speeds than those made of other materials.
5. Titanium: Due to its great strength, resistance to corrosion, and light weight, titanium has recently been employed for vital components such as motor shafts and bearings.
6. Ceramic: Due to its exceptional corrosion resistance and capacity to sustain high temperatures, ceramic bearings have been employed in EDFs.

We may anticipate more innovation and breakthroughs in the industry as materials science progresses, and it's conceivable that new materials will be created that are even better suited for EDFs.

History of Materials Used in The Past:

Hyfil, a carbon fiber material, was chosen by Rolls Royce in 1967 for the manufacture of the propeller blades and duct. The search for the ideal, more durable, and dependable material

for the fan never stopped. As a result, HexPly 8551-7, an amine-cured toughened epoxy resin system, was created in May 1970. When GE began using composites for non-ducted fans in the 1980s, it set the stage for the future growth of the aviation sector and an increase in propulsive efficiency. A preferred reinforcement resulted from the material innovation of graphite fiber. As carbon fiber promises strength, durability, and capacity to be 3D printed or machined into many forms and sizes, propeller blades have been made using it throughout history.
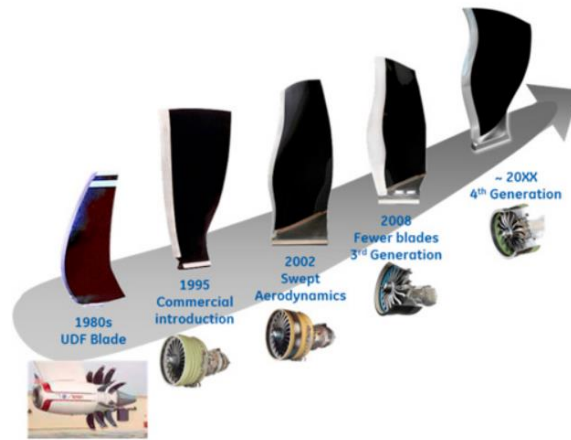
Figure 1: History of propulsion blades at GE

Comparison of Electric Ducted Fan with Gas-Powered Ducted Fan:

The energy produced by unleaded fuel in an internal combustion engine powers a gas-powered ducted fan. These engines provide energy, which powers the fan's motor. Due to its longer flying endurance and lack of need for pricey batteries and the time needed to recharge the batteries, a simple gas-powered ducted fan may be in higher demand. However, when it comes to size, portability, cost, safety, and noise reduction, electric ducted fans are a better option. We decide on an electric motor for a ducted fan instead of a gas-powered motor for the reasons listed below:

1. 1. A small UAV's weight and size are increased when a fuel tank is attached, which causes it to produce more thrust than is necessary.
2. 2. Li-Po batteries are less expensive than the gasoline needed to power ducted gas fans.
3. 3. Gas-powered ducted fans make noise, defeating their intended function of reducing propeller noise.
4. 4. A fan powered by an electric motor is simpler to service and maintain.
5. 5. If a UAV mishap occurs, it is extremely dangerous because it has a gas-powered ducted fan.
6. 6. Gas-powered UAVs are less mobile than EDF-equipped UAVs.

CHAPTER 2: LITERATURE REVIEW

The Not so much in the realm of research as it is in the field of engineering, the electric ducted fan (EDF) concept is new. Our team wanted to examine the various propulsion systems that were on the market and consider how to enhance them so that our FYP would both provide a deep learning experience and increase the effectiveness of propulsion systems. In addition, as we intended to produce this prototype locally in Pakistan, we also needed to consider whether manufacturing was feasible. In order to accomplish that, we first had to examine the various propulsion systems now in use and their diverse applications. The next step was to examine and contrast the different types of systems and consider the substantial benefits that an EDF would provide for us.

After accomplishing that, we had to explain how various ducted fan types differed and why an EDF was preferable to the alternatives. After gaining a basic understanding of the various propulsion systems, we needed to review the available literature on both propellers and ducts. After reading the pertinent literature, we would then concentrate on choosing the right batteries for the EDF. The review of the literature will be chronological and will go into detail on the relevant material that we looked at for each section.

Propulsion systems:

To understand the different types of propulsion systems, we first need to understand which application our EDF will be used for. Our standalone system was to be used to propel an **Unmanned Aerial Vehicle (UAV)/Drone for low flight capability.** Having this basic understanding, we will move forward.

Drones can be equipped with a wide variety of propulsion systems, depending on what the requirements are, pertaining to application, size, and design of the drone. Some of the common types of propulsion systems which are used as follows:

Electric Ducted Fans (EDFs):

> EDFs use electric motors to drive fan blades that are enclosed in a duct. They are powered by rechargeable batteries, and are known for their high efficiency, low noise, and ease of installation.

Figure 2: Electric Ducted Fan

Brushless Motors:

Brushless motors use magnetic fields to generate rotary motion and drive the propellers. They are widely used in drones due to their high power-to-weight ratio, low noise, and high reliability.

Figure 3: Brushless Motor

Internal Combustion Engines (ICEs):

ICEs use gasoline or diesel fuel to generate power and drive the propellers. They are commonly used in larger drones and unmanned aerial vehicles (UAVs) that require longer flight times and higher performance.

Figure 4: IC Engine

Hybrid Propulsion System:

Hybrid propulsion systems combine two or more different types of propulsion systems, such as an electric motor and a gasoline engine, to provide longer flight times and higher performance.
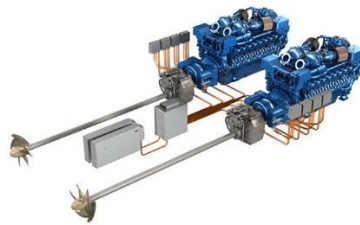
Figure 5: Hybrid Propulsion System

Multirotors:

Multirotors use multiple rotors to generate lift and propulsion, and are commonly used in small to medium-sized drones. There are several different types of multirotors, including quadrotors, hexacopters, and octocopters.

Figure 6: Multirotors

Turbojets:

A turbojet is a type of jet engine that uses a turbine to compress air and mix it with fuel, creating a high-speed stream of air that is expelled from the rear of the engine. This creates a forward thrust that propels the aircraft forward. Turbojets are widely used in military aircraft, commercial airliners, and some high-performance business jets.

Figure 7: Turbojets

RC Engines:

RC engines, or radio-controlled engines, are miniature engines used to power remote-controlled (RC) aircraft, such as RC planes, helicopters, and cars. RC engines are designed to be compact, lightweight, and powerful, and to provide the power needed for RC aircraft to perform a variety of maneuvers and aerobatic stunts.

Figure 8: RC Engine

Conclusion:

We decided to concentrate on propeller-driven systems alone from our list of propulsion technologies and then further investigate if it would be possible to produce an EDF in Pakistan. We first needed to examine the various forms of propulsion systems to understand why the EDF was not only more efficient but also more practical, and then we wanted to understand why we needed to focus primarily on propeller driven systems. We were also aware of the fact that our UAV was not particularly fast, did not weigh much, and was not carrying a heavy payload. We made the decision to limit our attention to small UAVs and propulsion systems employed in these drones, such as propeller-driven drones, ICEs, turbojets, RC engines, and EDFs.

In order to determine whether the duct offers us any noteworthy advantages, we first required to compare an EDF with an open propeller:

1. Better performance: Compared to open propellers, EDFs offer higher thrust-to-weight ratios, which can enhance the UAV's performance and manoeuvrability.

2. Quiet operation: Compared to open propellers, EDFs are very quiet, which is particularly advantageous for UAVs employed in noise-sensitive areas, such as during wildlife observation or aerial photography.

3. Increased safety: Since EDFs are powered by electricity, there is no chance of a fire breaking out or hot exhaust gases igniting, making them safer to use around people or in populated areas.

4. Greater efficiency: Compared to open propellers, EDFs are far more effective and can extend the UAV's flight time.

5. Increased dependability: Compared to open propellers, EDFs are often less complex and have fewer moving parts, which can make them more dependable and simple to maintain over time.

6. Less noise pollution: EDFs generate very little noise, giving them a more environmentally friendly option than open propellers, which generate a large quantity of noise pollution.

Once it has been determined that EDFs are more effective than open propellers in terms of their utilisation, we can contrast the EDF with alternative fuel-based propulsion methods.

1. RC engines and turbojets: They cost a lot to purchase, and it also costs more to maintain them. They must be shipped to the appropriate overseas manufacturer when they need maintenance because they often come from manufacturers situated abroad.

2. ICEs: The expense of running an ICE rises because we must use gasoline, and it also harms the environment more because the fuels utilised are frequently ones with high carbon contents. With regard to operational costs, a battery-based EDF will be less expensive than that. In addition to being rechargeable, the batteries have a longer lifespan than the typical ICE.

We now need to determine whether the EDF gives us a benefit over other fuel-based propellers after establishing why it is a superior option to other fuel-based propulsion systems and even open propeller-based systems.

Different propulsion technologies, such as electric ducted fans and fuel-based ducted fans, are employed by drones and other aerial vehicles. The source of power used to drive the fan is the key distinction between the two.

1. Electric ducted fans (EDFs): The fan blades of EDFs are driven by electric motors. They are renowned for their excellent efficiency and low noise levels and are powered by rechargeable batteries. Due to its minimal weight, simple installation, and low maintenance requirements, EDFs are frequently employed in small to medium-sized drones.

2. Fuel-Based Ducted Fans (FBDFs): The fan blades of FBDFs are propelled by internal combustion engines. They are recognised for their strong power-to-weight ratio and lengthy flight times, and are fueled by either petrol or diesel. Larger drones and UAVs that need more performance and longer flying periods frequently use FBDFs.

Performance-wise, FBDFs often deliver more power and have longer flying periods than EDFs, but they are also bulkier, noisier, and need more upkeep. EDFs, on the other hand, are less powerful and have a shorter range but are lighter, quieter, and more efficient.

The EDF will be a much better alternative for us because we need to create a unit that is not only lightweight but also efficient (because we are creating the EDF to power a small UAV with cruise capability for low flight situations).

Now that we have considered everything, we can state that, in some situations, Electric Ducted Fans (EDFs) have a number of benefits over open propellers, internal combustion engines (ICEs), turbojets, and RC engines:

1. Efficiency: EDFs have a high thrust-to-weight ratio and are very efficient, which makes them perfect for usage in small- to medium-sized drones.

2. Quiet Operation: EDFs are suitable for usage in noise-sensitive locations since they operate comparatively quietly in comparison to ICEs and turbojets.

3. Ease of Installation: EDFs don't require complicated exhaust or ducting systems because they normally consist of a single unit with a compact design that can be fitted into the drone.

4. Safety: Since EDFs run on electricity rather than dangerous fuels or hot exhaust gases, they are safer to employ in crowded areas and close to people.

EDFs are an environmentally beneficial substitute for ICEs and turbojets, which release greenhouse gases and other pollutants. They are powered by rechargeable batteries.

After examining various propulsion systems and the advantages the EDF offers, we now need to examine the many theories governing blade, propeller, and additional duct design because these will serve as the foundation for all of our analytical calculations.

Blade design:

To create a design for the EDF, we first needed to look at the design of a single blade, and the multiple theories surrounding that. For this, we reviewed multiple books, after which we found two key theories that were to be used: the disk theory/momentum theory, and the propeller theory. The disk theory would give us a preliminary understanding of what the propeller must look like, while the propeller theory talks about the parameters for selection of a single blade cross section, across which the entire blade will be built.

Disk Theory:

The disk theory of propellers is one of the theoretical models that we use to understand the aerodynamic properties of propellers, and is based on the assumption that we can model the complete propeller as a thin disk of negligeable thickness. We also assume that it moves at constant rotational speed through the fluid. The disk theory thus simplifies the analysis of propellers by assuming that the propeller blade is composed of infinite number of small blades that rotate around a central hub.
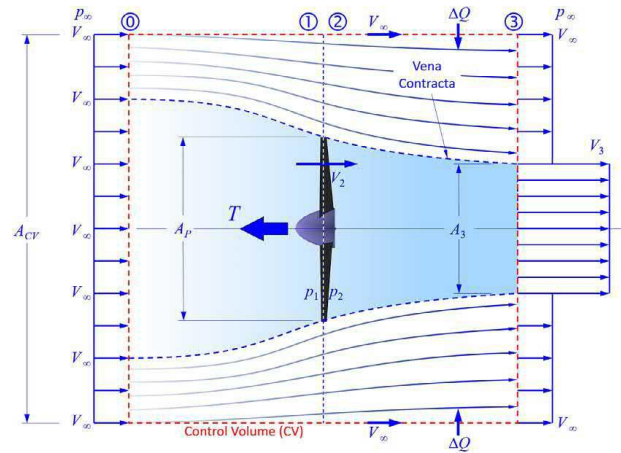
Figure 9: Disc Element Theory
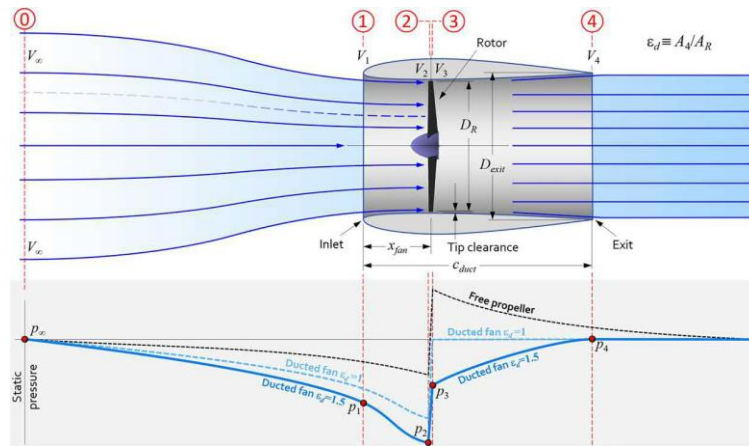
Figure 10: Static Pressure and Ducted Propeller Realtion

To understand the complete working of the theory, we also assume that the flow of air acts perpendicular to the disk surface. The propeller blades (in this case the disk), forces the air to rotate at high speeds, creating a pressure differential across the disk, causing a thrust and lift force. The magnitude of the lift and thrust generated by the propeller depends on several factors, including the blade angle, the rotational speed, and the air or fluid density.

While the disk theory is a simplified model of propeller aerodynamics, it provides a useful framework for understanding the fundamental principles of propeller operation. However, it is important to note that in reality, propellers are more complex than the simple disk model and their aerodynamic performance is influenced by a wide range of factors, including blade shape, blade twist, airfoil design, and the effects of compressibility and turbulence.

12

Blade Element Theory:

We then have the Blade Element Theory (BET) for propellers. This theory primarily looks at a single blade, dividing it into small, independent sections, called blade elements, with each blade element being seen as a thin, flat airfoil that produces lift and drag forces, when subjected to airflow. We then look at the lift and thrust performance of these airfoils, to choose which ones to select based on our requirements,
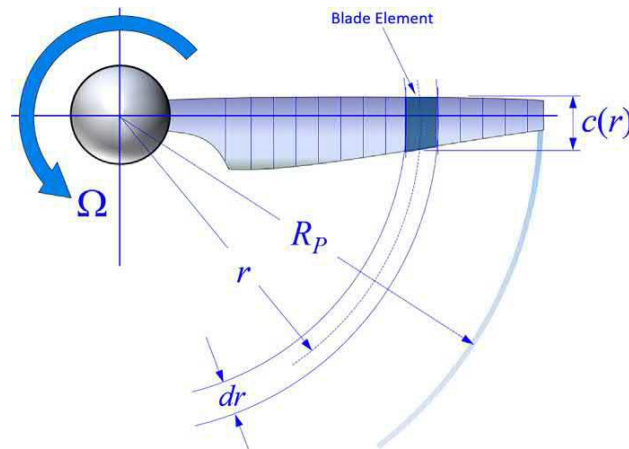
Figure 11: Section of a Blade

The premise of the blade element theory is that the airflow over each individual blade element can be individually examined, and the resulting forces may be added to determine the total performance of the rotor or propeller blade. The theory takes into account the local blade geometry, including chord length and twist angle, as well as the relative airspeed and angle of attack of each blade element.

The propeller or rotor blade is often separated into a number of sections along its length, with each section being independently analysed using airfoil data, such as lift and drag coefficients. This is done in order to apply the blade element theory. The total lift and drag forces produced by the propeller or rotor blade are then calculated by integrating the lift and drag forces operating on each portion along the length of the blade.

Engineers can now design rotors and propellers using the blade element theory, which has established itself as a common tool for this purpose. In order to analyse the aerodynamics of the turbine blades and maximise their efficiency, it has also been widely employed in the design of wind turbines.

Principal Performance Indicators:

We wanted to observe the critical design and performance characteristics in our design in order to comprehend the propeller's development and to fully comprehend the thrust capabilities of a complete propeller.

When creating a propeller, it's important to take into account the following design criteria:

1. Blade angle: The angle formed between the chord line of the blade and the plane of rotation is known as the blade angle. The thrust and lift the blade produces are determined by this angle.

2. Blade shape: The amount of lift and drag produced by the blade depends on the shape of the blade. The airfoil profile that is utilised to create the blade often describes its shape.

3. Blade pitch: If the blade were travelling through a solid medium, its pitch would be the amount it would advance throughout one rotation. It has an impact on how much push the blade produces.

4. Blade chord length: The blade's width parallel to the leading edge is referred to as the chord length. It has an impact on the lift and drag the blade produces.

5. Angle of Attack: The angle of attack is the relationship between the chord line and the direction of the relative airflow of an airfoil, such as a propeller blade. In a propeller, the twist of the blade and the shifting direction of the relative airflow as it passes through the blade cause the angle of attack to change along the length of the blade.

6. Blade twist: The variation in blade angle over the length of the blade is referred to as blade twist. It lessens the likelihood of stall and aids in maintaining an ideal angle of attack along the length of the blade.

7. Number of blades: The propeller's number of blades has an impact on how much push it produces. More blades generally produce more thrust, but they can also produce more drag.

8. Diameter: The diameter of the propeller influences how much air it can move, which in turn influences how much thrust it can produce.

9. Material: The propeller's weight, strength, and durability are all influenced by the material that it is made of.

Engineers can optimise a propeller's performance for a particular application, such as maximum thrust, efficiency, or noise reduction, by modifying these design characteristics.

Angle of Attack and Performance Relationship:

The angle of attack is important because it controls how much lift and drag the blade produces. As the angle of attack increases, the lift produced by the blade also rises until it reaches its maximum lift coefficient, after which the blade stalls and lift rapidly falls. Additionally, as the angle of attack increases, drag increases as well, which can lower the propeller's overall efficiency.

For a propeller to work at its best, the angle of attack must be optimised along the length of the blade. Typically, twisted blade designs that gradually alter the angle of attack along the length of the blade are used to achieve this. Engineers can optimise the angle of attack to create maximum lift and thrust while minimising drag and improving overall efficiency by altering the twist and other design parameters of the propeller blades.

Airfoil Types:

We then needed to look at the different types of airfoils that are frequently used in the industry, not only for propellers, but also for fixed wing UAVs. The two airfoil types we looked at were NACA and Clark-Y. The reason that we chose to look at these types of airfoils, was because we look at the relevant literature and research papers, and found these two to be the most suitable (as will be mentioned in later sections).

Using the characteristic curves that were available for these two airfoils, we then looked at what specific airfoils we could use, and their Cl vs Cd characteristics.

Choice of motor:

From the literature review that we conducted, we realized that motors can be categorized according to their different features, and use cases in propeller function. The two different ways we can categorize motors are as follows:

Brushless vs Non-Brushless: [1]

Brushless:

Brushless motors, also known as electronically commutated motors (ECMs), are a type of electric motor that does not use brushes for commutation. In traditional DC motors, brushes are used to transfer electrical current from the stationary part of the motor (stator) to the rotating part of the motor (rotor), which generates torque and rotational motion.

In a brushless motor, the commutation is done electronically through the use of a controller that switches the current flowing through the stator coils in a precise sequence, based on the position of the rotor. The rotor contains permanent magnets that interact with the

electromagnetic fields generated by the stator coils, which creates torque and rotational motion.

Non-brushless:

Non-brushless motors typically refer to traditional brushed motors, which use brushes to transfer electrical current from the stationary part of the motor (stator) to the rotating part of the motor (rotor).

In a brushed motor, the commutation is done mechanically through the use of carbon brushes that come into contact with the commutator on the rotor. As the rotor rotates, the brushes switch the electrical current flowing through the motor windings, creating torque and rotational motion.

Comparison:

Brushed motors have several disadvantages compared to brushless motors, including lower efficiency, shorter lifespan due to brush wear, and limited speed control capabilities. However, they are still commonly used in applications that require low-cost, simple motor solutions with lower performance requirements, such as small consumer electronics, toys, and some automotive applications.

In comparison, brushless motors offer several advantages over traditional brushed motors, including higher efficiency, longer lifespan, higher power density, and better speed control. They are commonly used in applications that require high performance, reliability, and efficiency, such as drones, electric vehicles, and industrial machinery.

Inrunner vs Outrunner: [2]

Inrunner:

Inrunner motors are a type of brushless DC motor in which the stator is located on the outside of the motor and the rotor is located on the inside, hence the name "inrunner". In other words, the rotor rotates inside the stator.

In inrunner motors, the rotor is typically mounted on a shaft that runs through the center of the motor and is supported by bearings. The stator consists of multiple stationary windings that are located around the outside of the motor. When current is applied to the windings, an electromagnetic field is generated that interacts with the permanent magnets on the rotor, creating torque and rotational motion.

Figure 12: Inrunner Motor

Outrunner:

Outrunner motors are a type of brushless DC motor in which the stator is located on the inside of the motor and the rotor is located on the outside, hence the name "outrunner". In other words, the stator is fixed and the rotor spins around it.

In outrunner motors, the rotor typically consists of a cylindrical casing that rotates around the stator. The casing contains multiple permanent magnets that interact with the electromagnetic field generated by the stationary windings on the stator, creating torque and rotational motion.

Figure 13: Outrunner Motor

Comparison:

Outrunner motors are generally larger and heavier than inrunner motors but have higher torque and are more efficient. They are commonly used in applications that require high torque and low speed, such as electric bicycles, industrial machinery, and model airplanes. They can also be used in high-speed applications, although they may not be as efficient as inrunner motors in these cases.

Inrunner motors are typically smaller and lighter than their counterpart, the outrunner motor, and are commonly used in high-speed applications such as drones, RC cars, and other model vehicles. However, they generally have lower torque and are less efficient than outrunner motor.

Conclusion:

The conclusion we came to was that we need to select a Brushless DC motor (BLDC), however, whether it is an inrunner or outrunner will depend on the specific RPM that we will require.

CHAPTER 3: METHODOLOGY

Design Methodology:

In the beginning, the only design parameters set were the thrust and speed of the aerial vehicle. From the literature review and conceptual design, we were able to fix some of the other parameters like the rotational speed of the propeller and the Reynolds Number.

The design of the ducted propeller was done in two steps, the first was the design of the propeller that is able to produce the required thrust and then designing the duct around it to reduce the power requirements.

Before diving into designing the propeller, it is needed to fix the diameter of the propeller. This could be done in two ways. We can select an approximate size using our trade study and make calculations on its basis, or we can use the formulas provided in the literature[3] to calculate the size of the free propeller. The latter choice seems more appropriate as it's based on literature. The formula to calculate the diameter of the propeller is given by

$$D_p = K_p \sqrt[4]{P_{BHP}}$$

Using K_p value from literature and power from

$$P = T \times V_\infty$$

Where, V_∞ is the cruise velocity and T is the required thrust. Using the set values the diameter of initial design was fixed as 20 inches. From our study we also fix the size of the hub to be $0.2D_p$.

Design of the propeller:

For designing the propeller, we used a combination of the two theories covered in the literature review i.e., the *'momentum theory'* also known as the disk theory and the *'blade element theory (BET)'*.

Using the BET[4], we first design a single blade. The blade element theory estimates the thrust of a propeller by dividing the blade into several segments, called *blade elements*. Each element is treated as an independent two-dimensional airfoil. By doing this, aerodynamic forces of lift and drag are calculated based on local conditions at each of these blade elements. Once the forces are determined, they are summed to represent the properties of a complete blade. These are then multiplied with the total number of blades of the propeller to get the properties of the propeller.
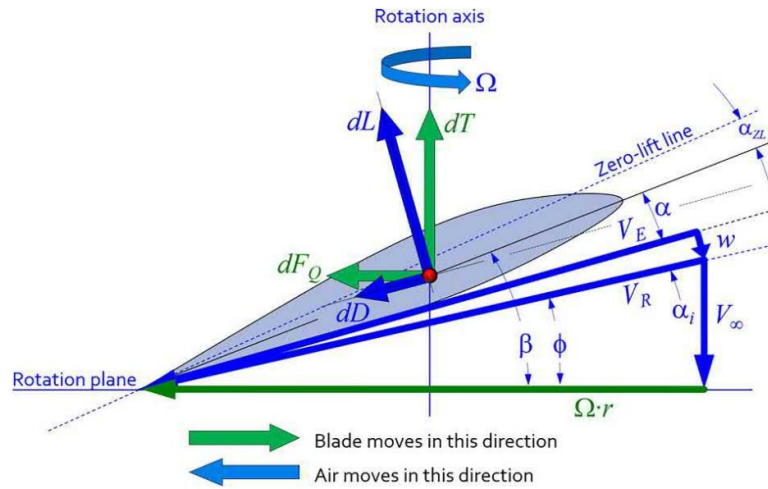
Figure 14: Forces, angles, and velocity for an airfoil of propeller blade [5]

The differential lift and drag forces of the elements dL and dD are as follows:

$$dL = \frac{1}{2}\rho V_E^2.c(r).C_l.dr$$

$$dD = \frac{1}{2}\rho V_E^2.c(r).C_d.dr$$

Where,

r = Arbitrary distance from hub to blade element

V_∞ = Forward airspeed of the aerial vehicle

V_E = Effective resultant velocity

V_R = Resultant velocity

w = Elemental induced velocity

Ω = Angular velocity of the propelle

α = Elemental angle-of-attack

α_i = Induced AOA

β = pitch angle

ϕ = Helix angel

Once elemental lift and drag are known, the differential thrust, torque, and power can be calculated as follows,

Elemental thrust:

$$dT = dL\cos(\varphi + \alpha_i) - dD\sin(\varphi + \alpha_i)$$

Elemental torque:

$$dQ = r.dF_Q = r[dL\cos(\varphi + \alpha_i) + dD\sin(\varphi + \alpha_i)]$$

Elemental Power:

$$dP = \Omega r.dF_Q = \Omega r[dL\cos(\varphi + \alpha_i) + dD\sin(\varphi + \alpha_i)]$$

The blade is divided into 16 elements, each $0.05r$ apart. At first the elemental thrust, torque, and power are calculated for the element at $0.75r$. Each of the parameter needed for these calculations is determined as follows:

Selection of an airfoil: [6]

Before we start calculating the parameters required to measure thrust produce by an element of blade, we need to select an airfoil. Each blade is made of multiple airfoils with different cord lengths and blade angles stacked together.

Several literatures[7][8] propose the use of NACA4412 for propeller blades because of it good performance in low and high speed. So, we took NACA4412 as a benchmark for comparison and saw different propellers with similar characteristics.

Table 1: Airlfoil Comaprison

Compan y name	S.No	Airfoil Name	AoA for min Cd	AoA for lift stall	Cl/Cd	AoA (max Cl/Cd)	Cl/Cd for recommende d AoA	AoA (recommende d)
					Airfoil Selection			
NACA	1	NACA-4412	0	9	36.1	8.5	20	2
	2	NACA-4418	0	10	23.06	5.75	18	2.5
	3	NACA-0009	0	8	25.59	4	18	2.5
	4	NACA-0012	2.5	10	26.54	5.5	10	1
	5	NACA-2410	-2	11	36.08	6	23	2.5
	6	NACA-2415	2.5	11	31.41	7.5	23	2.5
Clark -	1	(clarkv-il) CLARK V AIRFOIL	-2	8 to 12	35.49	8	35.49	8
	2	CLARK-Y 11.7	-2 to 7.5	10 to 15	35	8	27.5	2
	3	CLARK YS AIRFOIL	-2.5 to 7.5	8	31.7	7.25	30	5

From comparison we saw the maximum lift to drag ratio was in fact given by NACA4412. At this point the performance of propeller is maximum. However, this angle if very close to stall, and a small change in angle of attack can lead to drastic increases in drag. So, we compromise to find minimum drag while having significant coefficient of lift. From observing the graphs of coefficients vs angle of attack, we select the best angle of attack given our consideration. Looking at C_l/C_d ratio at this new angle of attack, we see the maximum ratio is give by **CLARK-Y 11.7**. Its shape is also similar to the our benchmark airfoil. So, CLARK-Y 11.7 is selected as the airfoil. The coefficients of lift, drag and their ratios against the angle of attack are shown in figure 2. These values are at Reynolds number 100,000 which was fixed from the literature.
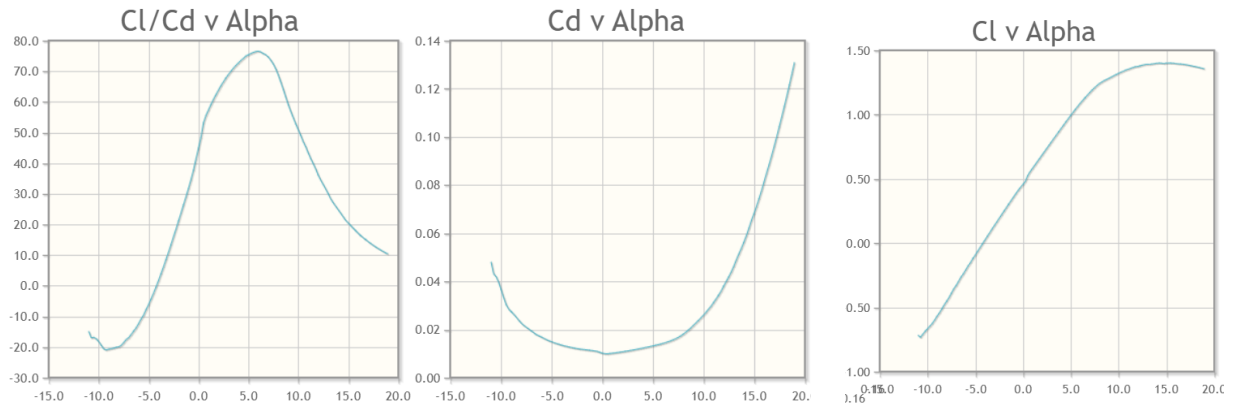
Figure 15: Coefficients of lift and drag, and their ratio as a function of angle of attack.

Distance from hub to blade element, r:

r is the distance from the center of hub to the blade element at which we are trying to find the parameters. Since the first element we select is at 75% radius of the propeller, the value of r is given by:

$$r = 0.75R$$

We have divided the blade into 16 elements so we will find the required parameters at 0.2, 0.25, 0.3, 0.35, ………, 1 of the propeller's radius.

Forward air speed of the aerial vehicle, V_∞:

V_∞ is the forward speed of the bird in cruise condition. The propeller is being designed for a bird that is cruising with a speed of 20 m/s.

Angular velocity of the propeller, Ω:

The rotational velocity of the propeller is set from literature. In the initial design the propeller is rotating at a speed of 5000 rpm.

Resultant Velocity, V_R:

Resultant velocity is the total velocity of the airfoil at each blade element. It can also be thought of as the velocity with which air strikes the airfoil if there is no induced velocity. Resultant velocity is the vector sum of forward air speed of the bird and the tangential velocity due to rotation at the location. It is given by:

$$V_R = \sqrt{V_\infty^2 + (\Omega r)^2}$$

23

Induced velocity, w:

The induced velocity is the change in the air velocity due to aerodynamic interaction with the blades of the propeller. The momentum theory is used to determine the induced velocity. Using momentum theory we equate following expression:

$$f(w) = \frac{8\pi r}{N_B.c(r)}w - \sqrt{1 + \frac{(\Omega r)^2}{V_\infty + w}[C_l.(\Omega r) - C_d.(V_\infty + w)]}$$

The root of this function gives us the value of induced velocity. To find the roots we implement a Newton-Raphson iterative scheme.

Effective velocity, V_E:

Effective velocity is the velocity with which air strikes the blade element of the propeller. It includes the effect of induced velocity, w as well. The effective resultant velocity can be estimated:

$$V_E = \sqrt{(V_\infty + w)^2 + (\Omega r)^2}$$

V_E is the velocity used to calculate the aerodynamic forces of lift and drag.

Chord length, c:

Chord length of the airfoil can be determined from the following relation:

$$Re = \frac{V_E.c}{v}$$

The Reynolds number is fixed from the literature, and the value of kinematic viscosity is known. Thus, the chord length of the airfoil is calculated.

Angle of Attack, α:

Angle of attack is the angle between the incoming air velocity vector and the chord length. The value of drag and lift coefficient depends on the angle of attack with which air approaches the airfoil.

At the selection of airfoil, the value of angle of attack is also fixed that gives us the best results. For CLARK-Y 11.7%, the best results were obtained at an angle of 2 degrees.

Helix Angle, φ:

The angle between the rotational plane and the circumference $2\pi r$ at each blade station is called helix angle. In simpler words, it is the angle the resultant velocity substituted with the plane of rotation. Helix angle at blade station r is calculated using the following expression:

$$\varphi = \tan^{-1}\frac{V_\infty}{\Omega r}$$

Induced Angle of Attack, α_i:

α_i is the angle of attack induced by w. Knowing induced velocity, w the induced angle of attack can be estimated from:

$$\alpha_i = \sin^{-1}\frac{w}{V_R}$$

Geometric Pitch Angle, β:

Also known as the blade angle, geometric pitch angle is the angle at which we set the airfoil to be stacked to form a complete blade. It is the angle between chord line and the plane of rotation. The blade angle is maximum at the hub and decreases as we move toward the tip. It is usually given as the sum angle of attack, induced angle of attack, the helix angle.

$$\beta = \alpha + \alpha_i + \varphi$$

Now all the angles, velocities, and other parameters are determined, the aerodynamic forces can be calculated.

Elemental Lift, dL:

The component of aerodynamic force that acts perpendicular to the direction of velocity is called lift force. The elemental lift of a blade station r is given by

$$dL = \frac{1}{2}\rho V_E^2.c(r).C_l.dr$$

Elemental Drag, dD:

The component of aerodynamic force that acts parallel to the direction of velocity is called lift force. The elemental drag of a blade station r is given by

$$dD = \frac{1}{2}\rho V_E^2 . c(r) . C_d . dr$$

Knowing the aerodynamic forces, the elemental thrust, torque, and power can be calculated. by the relations given above at the start of this section.

Once the elemental parameters are calculated, these are summed to get the properties of one complete blade. The total thrust, torque, and power can then be found.

Thrust, T:

$$T = N_B \int_{R_{hub}}^{R} dT$$

$$T = N_B \left| \int_{R_{hub}}^{R} dL\cos(\varphi + \alpha_i) - \int_{R_{hub}}^{R} dD\sin(\varphi + \alpha_i) \right|$$

Torque, Q:

$$Q = N_B \int_{R_{hub}}^{R} r . dF_Q$$

$$Q = N_B \left| \int_{R_{hub}}^{R} r . dL\sin(\varphi + \alpha_i) + \int_{R_{hub}}^{R} r . dD\cos(\varphi + \alpha_i) \right|$$

Power, P:

$$P = N_B \int_{R_{hub}}^{R} \Omega r . dF_Q$$

$$Q = N_B \left| \int_{R_{hub}}^{R} \Omega r . dL\sin(\varphi + \alpha_i) + \int_{R_{hub}}^{R} \Omega r . dD\cos(\varphi + \alpha_i) \right|$$

Initial Design of the Propeller:

In the initial design, with 3 blades, 0.508 m radius, Reynolds number 100000, 5000 rpm, and cruise velocity of 20 m/s the thrust, torque, and power came out as follows:

$$T = 33.7 \, N \qquad ; \qquad Q = 2.67 \, Nm \qquad ; \qquad P = 1.4 \, kW$$

This satisfies the requirement of a 3 kg thrust.

Since the chord lengths of each of the 16 elements and their blade angles were calculated, these values are used to make the initial design of the propeller in a CAD/CAM software.

After modeling in Solidworks, the initial design of the propeller giving us the thrust, torque, and power values mentioned above is:
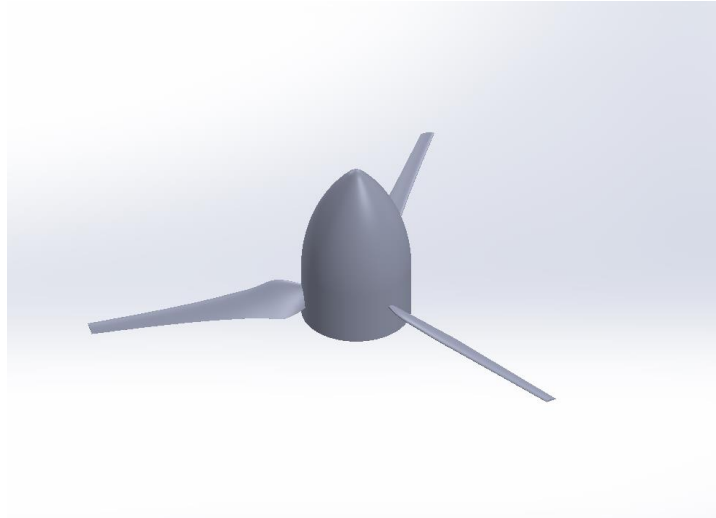
Figure 16: 3D view of Initial Design
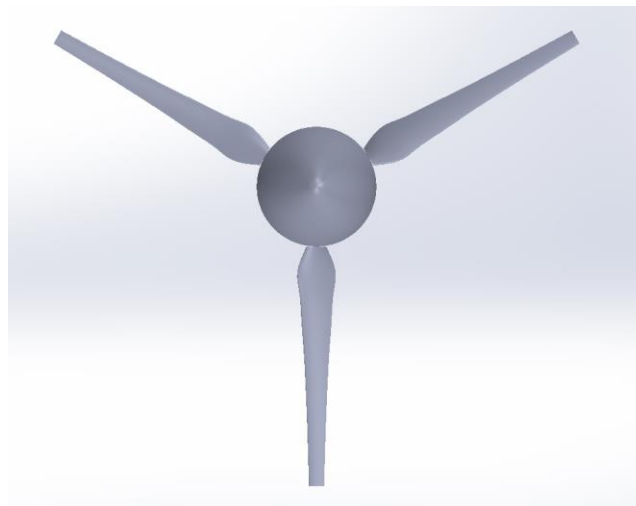
Figure 17*:* Top view
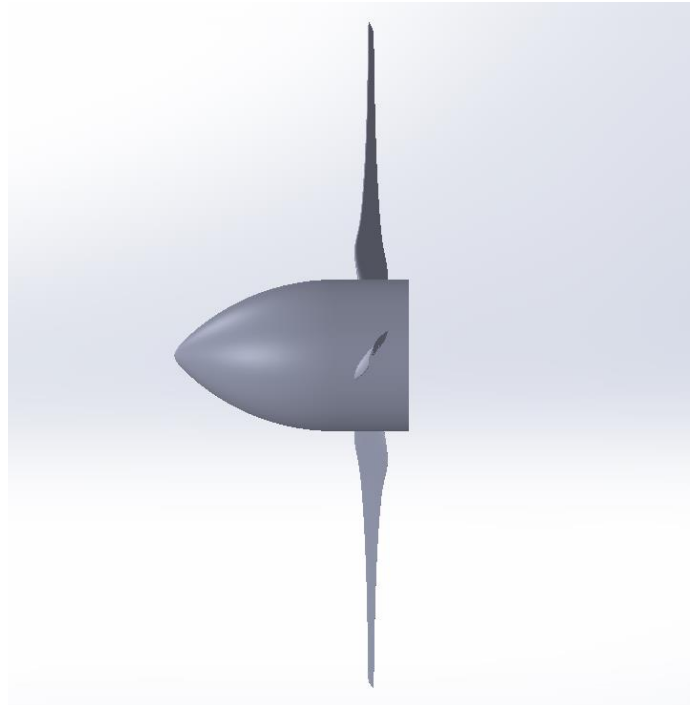
Figure 18: Side view

Problems with design:

The initial design on solidworks show that the blades are very thin. This might arise two problems for us. First, thin blades are difficult to manufacture and the height of airfoil especially at tip is under the minimum dimensions that can be 3D printed. If we later on choose to use 3D printing as mode of manufacturing, the tips will not be manufactured accurately. The second problem is that the blades will not be able to withstand the stresses produced upon thrust generation and might bend.

The reason blades are thin is because we are using a very big diameter propeller relative to the value of thrust it is producing. Initially, the diameter was calculated based on a formula provided by literature. Now, we will use the other technique of fixing the diameter from trade study of propellers of the producing similar thrust. From trade study it is seen that for 3 kg thrust, the propellers are usually 10 – 15 inches. 12 inches was selected as the new value of diameter and repeat the process. This time Reynold's number is taken as 200,000 and the rest of the initial set conditions are kept the same. Using these as initial parameter, with 4 blades, 0.3048 m radius, Reynolds number 200000, 5000 rpm, and cruise velocity of 20 m/s, the results are as follows:

$$T = 30.1\ N \qquad ; \qquad Q = 2.62\ Nm \qquad ; \qquad P = 1.37\ kW$$
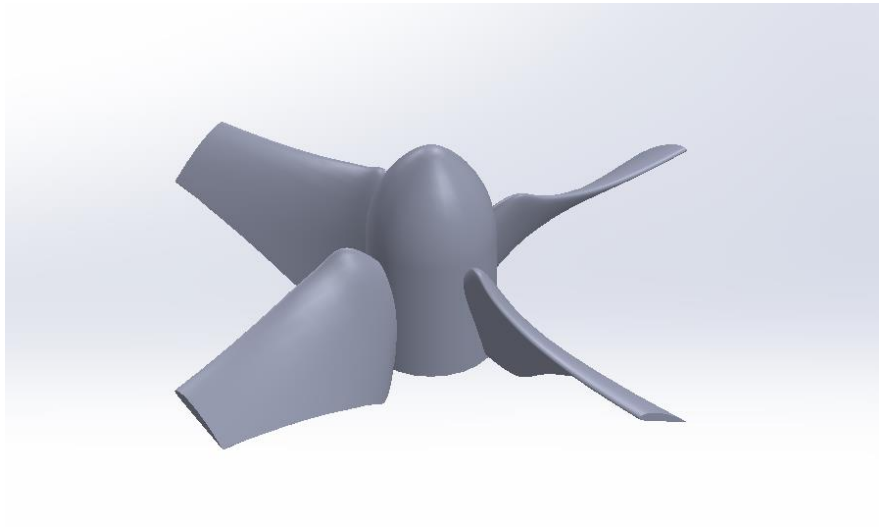
Figure 19: 3D view of Design
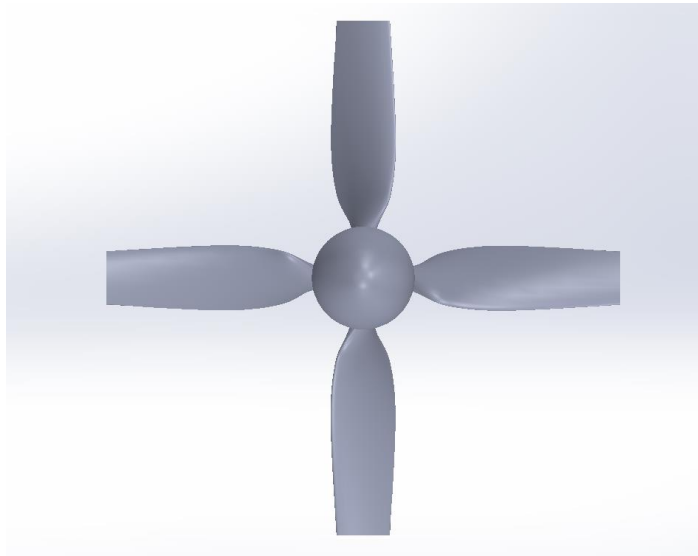
Figure 20: Top view
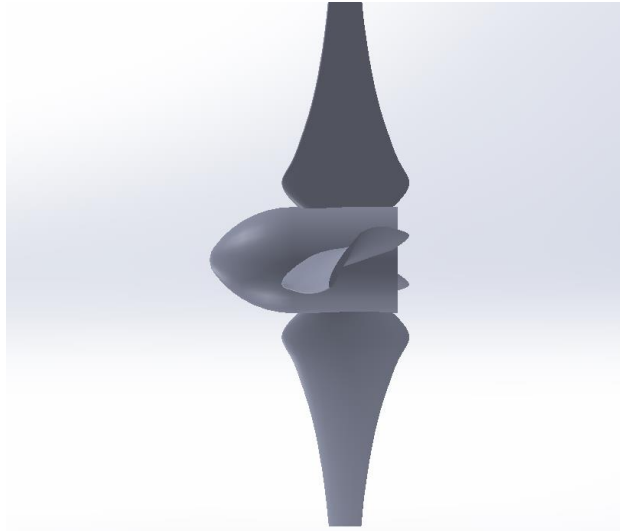
Figure 21: Side view

Design of the duct:[9]

The ducts have exit area larger than the prop's disc area. This increase in area for air leaving the propeller's blades reduces the exit velocity and increases the mass flow producing greater thrust. Thus, less power is required for same thrust generation. The change in area is expressed in terms of diffuser expansion ratio, ε_d, defined as the ratio between exit area A_{exit} and rotor disc area A_R.

$$\varepsilon_d = \frac{A_{exit}}{A_R}$$

The diffusion expansion ratio is the most effective design parameter for the ducted propeller. The value of diffusion ratio was selected as 1.247. This selection was based on iterative method until we achieved the value of power desired for thrust generation.

The other parameters to consider while designing the duct are

Rotor Area, A_R:

Rotor area is the area of the duct at the cross-section where the propeller is located. It is calculated from the propeller's radius plus the tip clearance.

Tip clearance:

The tip clearance is the distance between the radius of propeller and the inner radius of the duct where the propeller is located inside the duct. It is the space between the blade tip and duct wall. The smaller the tip clearance is the more efficient is the performance of the duct.

Greater tip clearances will increase the tip losses. Usually, the tip clearance should be between 1 to 3 mm[10]. For designing the duct, 2 mm tip clearance was selected.

Induced speed, w:

$$w = \left(\frac{1}{2}\varepsilon_d - 1\right)V_\infty + \sqrt{\left(\frac{\varepsilon_d V_\infty}{2}\right)^2 + \frac{\varepsilon_d T}{\rho A_R}}$$

Airspeed through the rotor, V_R:

The velocity with which the air leaves the blades. It is given by,

$$V_3 = V_\infty + w = \frac{\varepsilon_d V_\infty}{2} + \sqrt{\left(\frac{\varepsilon_d V_\infty}{2}\right)^2 + \frac{\varepsilon_d T}{\rho A_R}}$$

Airspeed at the exit, V_{exit}:

This is the velocity of air leaving the duct, and is expressed as,

$$V_{exit} = V_\infty + \Delta V = \frac{V_R}{\varepsilon_d}$$

Power, P:

In case of ducted propeller, less power is required to generate the same thrust compared to open propeller. The required power in this case is given by,

$$P_{req} = \frac{3}{4}TV_\infty + \sqrt{\frac{T^2 V_\infty^2}{4^2} + \frac{T^3}{4\rho A_R \varepsilon_d}}$$

For the propeller designed in the above section, if a duct with a diffusion ratio of 1.247 is placed around it with ta ip clearance of 2 mm, the power is reduced to **721.5 W**. Thus, the power requirement is reduced by 47%. After adding the stators, the final design of the duct for the propeller on Solidworks came out as shown below.
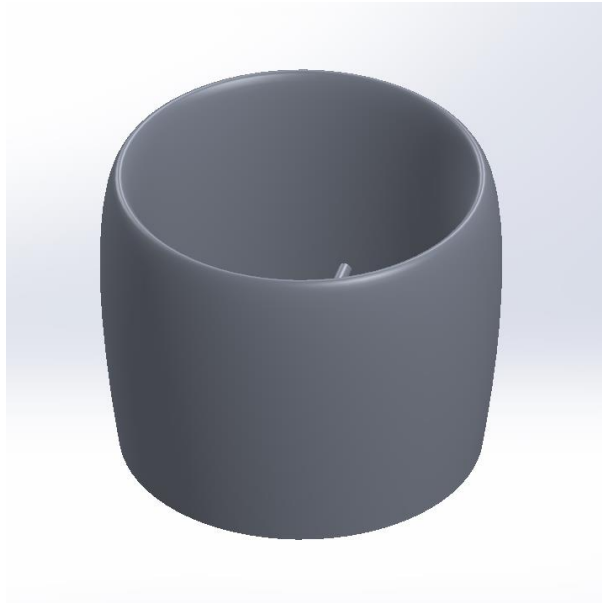
Figure 22: 3D view of the duct
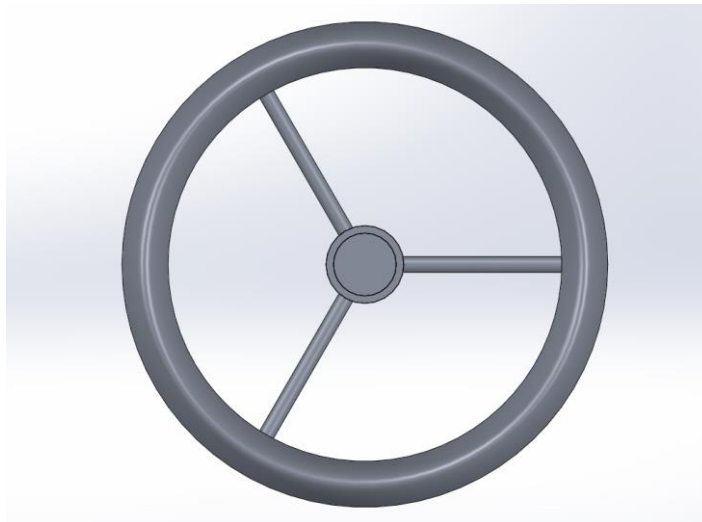
Figure 23: Top view of the duct
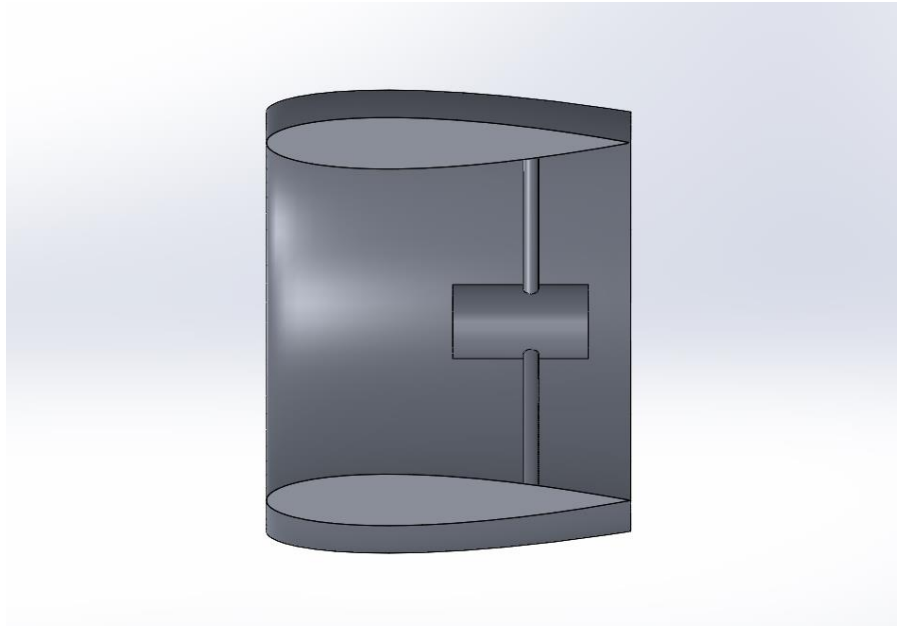
Figure 24: Cross-sectional side view

Prototyping:

Propeller:

Based on the 3-D design that we developed, along with the CFD modeling that we did, we had a finalized design that we could use for our actual model. This was then 3-D printed, with ABS being the 3-D print material that we used. It is important to note, that we printed the hub, and all of the propeller blades in one go.

Figure 25: 3-D printed ABS fan

Since it was impossible to attach the hub directly to the motor, we had to attach a shaft from the motor, through the hub of the propeller. For this purpose, we drilled a hole through the hub, however, due to the propeller being 3-D printed, this caused us significant issues initially as the hub is hollow from within, and would cause unnecessary motion of the shaft once the motor would rotate. To fix this issue, we attached flanges on both sides of the hub, and the shaft was press fitted through the hub, with a internally tapered stopper cap attached to the front of the hub. This prevented the shaft from vibrating excessively as we increased the RPMs of the motor.

Figure 26: Flanges and shaft

After this we had to focus on balancing of the propeller. We know that material is not equally distributed across a design during 3-D printing, whereby one of the blades might be heavier than the rest. This would once again cause excessive vibrations as the propeller rotates at high RPMs. To avoid this, we balanced the propeller on two circular, smooth shafts placed on equal heights, and let the propeller rotate on its own, until it becomes stable. During this process, we will see the propeller fall over in one direction, which would indicate that the weight of that particular blade is greater than the rest of the blades. Based on this conclusion, we kept on adding tape to the specific propeller blades to counterbalance the blades with added weight (since our propeller was 3-D printed, it had very minimal mass, which meant adding small strips of tape would help add the necessary counterweights).

Figure 27: Balancing of fan

Motor Housing:

We also needed a stable housing for the motor to be placed in. This was done so as to:

i.   Fix the open propeller with the stable supports on the test bench.
ii.   Fix the motor with the static supports within the duct

The motor housing was also made from 3-D printed ABS, and the motor was fitted into the housing. The housing also provided static support to the motor, and dampened any excessive vibrations produced by it during its motion.

Figure 28: Motor housing

Test Bench:

To measure the thrust, we had decided to mount both the open propeller, and the ducted propeller on static supports, and these supports were then to be mounted on moving sliders[11]. The slider blocks would be free to move on rails, which would be fixed on a wooden board. Behind our prototype, we had a fixed support, where one end of the force balance would be attached. The other end of the force balance would be attached to the motor housing that we had 3-D printed. As the motor is turned on, and the EDF starts generating thrust, the force would be recorded by the force balance. Our static supports were also made from 3-D printed PLA (since we did not need very high strength capability here).
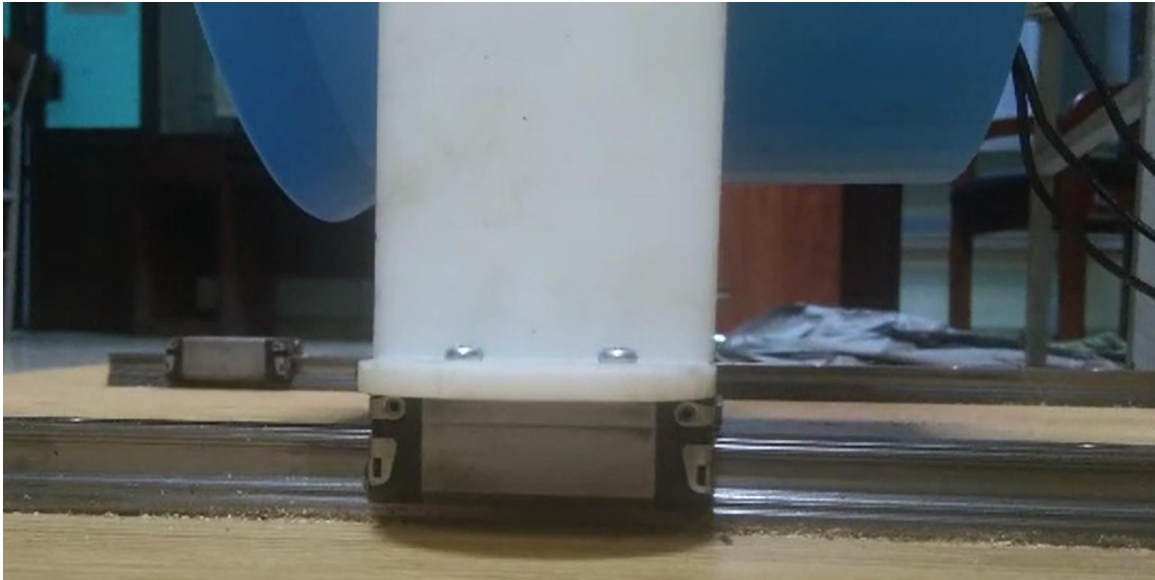
Figure 29: Static supports and sliders for test bench

Electrical Components:

Based on our thrust requirement, number of blades, and hub diameter, we first selected our motor based on the characteristic charts we received for our specific motor. Alongside the motor, we used the recommended ESC. On the output of the ESC, we attached an RC servo tester to adjust the speed of the motor, so as to have the capability to run the EDF on different RPMs.

Along with this, we also used two 3S LiPo batteries in series (so a 6S battery), as it provided us with the required power input.
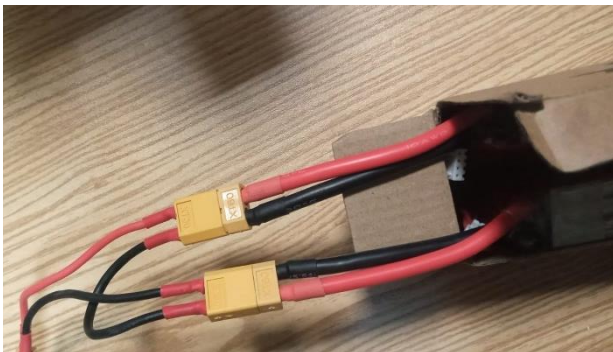
Figure 31: Two 3S LiPo batteries in series

Figure 30: RC Servo Tester

Motor selection:

We based our selection on the following criteria:

Design Integration: The diameter of the motor should be significantly less than that of the hub (less than 0.2*12*25.4mm). This is so the motor including the housing that we build for it stay within the hub diameter.

Aerodynamic Requirements: The motor should be able to reach our desired 5000RPM at full throttle. It is hard to estimate this without motor performance curves and other data which were not available from manufacturers. We therefore looked at motors that had a fairly high no load RPM than our RPM requirement and deliver thrust around our requirement (3kg) using a similar sized propeller or bigger, at full throttle.

Cost and availability: The cost and availability were two big factors. Due to import bans, we had to make sure we could procure our motor from a well-reputed local vendor.

Considering all of the aforementioned reasons, we decided to select the "*Gartt ML 5210 340kv 4600gram 4.6kg thrust Brushless motor.*"

Figure 32: Gartt motor (Rs. 11,200: Cheaper)

Figure 33: T-motors AM600 motor ($129: more expensive)
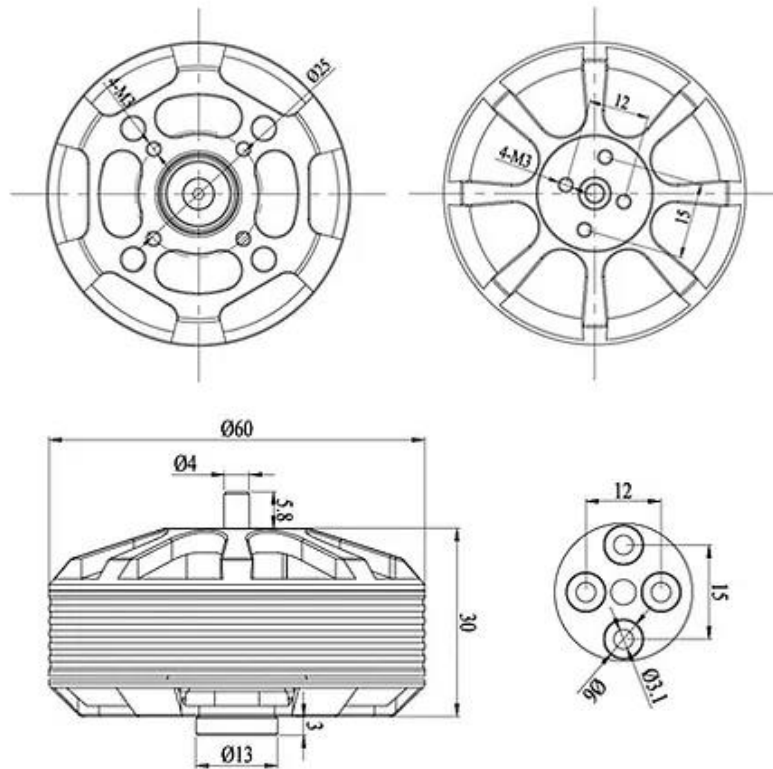
Figure 34: Motor dimensions

We can also see the data available within the following performance charts. As we can see, not only did we consider the torque and RPM required, we also looked at the optimum number of blades that the motor can ideally support:

ML5210								
Item NO.	Volts (V)	Prop	Throttle	Amps (A)	Watts (W)	Thrust (g)	Efficiency (g/W)	Operating temperature (℃)
ML5210 340KV	24V	1555	50%	3.6	86.4	870	10.07	40℃
			54%	5	120.0	1100	9.17	
			57%	6	144.0	1260	8.75	
			62%	8	192.0	1530	7.97	
			66%	10	240.0	1800	7.50	
			70%	12	288.0	2050	7.12	
			76%	14	336.0	2280	6.79	
			79%	16	384.0	2510	6.54	
			81%	18	432.0	2740	6.34	
			100%	20	480.0	2920	6.08	
ML5210 340KV	24V	1755	50%	5.3	127.2	1230	9.67	61℃
			53%	8	192.0	1640	8.54	
			59%	10	240.0	1910	7.96	
			62%	12	288.0	2150	7.47	
			69%	14	336.0	2410	7.17	
			68%	16	384.0	2620	6.82	
			71%	18	432.0	2850	6.55	
			76%	20	480.0	3030	6.31	
			77%	22	528.0	3260	6.17	
			79%	24	576.0	3420	5.94	
			82%	26	624.0	3610	5.79	
			100%	28.3	679.2	3830	5.64	
ML5210 340KV	24V	1855	50%	6.8	163.2	1510	9.25	73℃
			52%	8	192.0	1720	8.96	
			55%	10	240.0	2040	8.50	
			58%	12	288.0	2210	7.67	
			61%	14	336.0	2480	7.38	
			63%	16	384.0	2670	6.95	
			66%	18	432.0	2910	6.74	
			68%	20	480.0	3120	6.50	
			70%	22	528.0	3330	6.31	
			73%	24	576.0	3510	6.09	
			79%	26	624.0	3660	5.87	
			78%	28	672.0	3840	5.71	
			80%	30	720.0	3950	5.49	
			82%	32	768.0	4070	5.30	
			100%	34.2	820.8	4180	5.09	
ML5210 340KV	24V	2055	50%	7.1	170.4	1600	9.39	73℃
			52%	8	192.0	1750	9.11	
			53%	10	240.0	2070	8.63	
			57%	12	288.0	2250	7.81	
			60%	14	336.0	2520	7.53	
			62%	16	384.0	2730	7.11	
			64%	18	432.0	2980	6.90	
			68%	20	480.0	3200	6.67	
			69%	22	528.0	3410	6.46	
			71%	24	576.0	3590	6.23	
			73%	26	624.0	3710	5.95	
			76%	28	672.0	3900	5.80	
			78%	30	720.0	4090	5.68	
			80%	32	768.0	4210	5.48	
			100%	36.1	883.2	4620	5.23	

Notes: The test condition oftemperature is motor surface temperature in 100% throttle while the motor run 10 min, environment temperature 26℃.

Figure 35: Gartt Performance charts [12]

ML5210 MOTOR/340KV

Motor KV--------------------------------340KV RPM/V

Motor Resistance (RM)-----------------------0.0622 Ω

Idle Current (Io/10V)------------------------0.7A/10V

Max Continuous Current --------------------------40A

Max Continuous Power---------------------------960W

Weight--------------------------------≈230g/8.11oz

Lipo Cell------------------------------------6S-8S

Motor Diameter-------------------------60mm/2.36in

Motor Body Length----------------------30mm/1.18in

Configu-ration--------------------------------24N22P

Overall Shaft Length-------------------36.7mm/1.44in

Shaft Diameter-------------------------4.0mm/0.157in

Bolt holes spacing-----------------------25mm/0.98in

Bolt thread-------------------------------------M3×8

Figure 36: Gartt specs [12]

CHAPTER 4: RESULTS AND DISCUSSIONS

**Results from Analytical Calculation:**

Propeller Diameter:

Propeller diameter is a crucial factor that affects the performance of an electric ducted fan. A larger diameter propeller generates greater thrust, which is required to lift heavier loads. Also increasing the diameter of the propeller also increases its weight and drag, reducing the efficiency of the fan. On the other hand, reducing the diameter of the propeller reduces its weight and drag, increasing the efficiency of the fan. The exact choice of diameter is done by considering the UAV as our EDF is designed for a small UAV so we selected a 0.3048 m diameter of the propeller. This will not increase the weight of the EDF so the size is kept such that it will provide enough thrust and strength to carry the load forces of a small UAV in which it is going to be installed and the space available for installation.

Propeller Pitch:

It is another important parameter that affects the performance of an electric ducted fan. The pitch of the propeller refers to the angle at which the blade is set, and it has a significant impact on the performance of the fan. The propeller pitch is set such that the angle of attack of wind encountered by the blade remains as near to the ideal angle of attack as possible, ensuring that the blade generates the maximum amount of thrust throughout its span and doesn't stall at any point along its length. We have chosen a constant pitch propeller where the angle of attach α is 2°.

Chord Length:

Chord length is the third parameter that is discussed in the document. It is the length of the cross-section of the blade, and it has a direct impact on Reynold's number, which is a dimensionless quantity used to determine the level of turbulence in fluid flow. Longer chord length results in a higher Reynold's number, indicating a higher level of turbulence in the fluid flow. This increased turbulence can result in a reduction in the efficiency of the fan, as it generates more drag and requires more power to rotate. On the other hand, a shorter chord length results in a lower Reynold's number, indicating a lower level of turbulence in the fluid flow. This reduction in turbulence can increase the efficiency of the fan, as it generates less drag and requires less power to rotate. Therefore, the chord length was analytically calculated on the basis of effective velocity, dynamic viscosity, density and Reynold's Number. The blade shape changes as the length of the chord length change for a Clark Y 11.7% smooth airfoil.

CHORD LENGTH OVER LENGTH OF THE BLADE
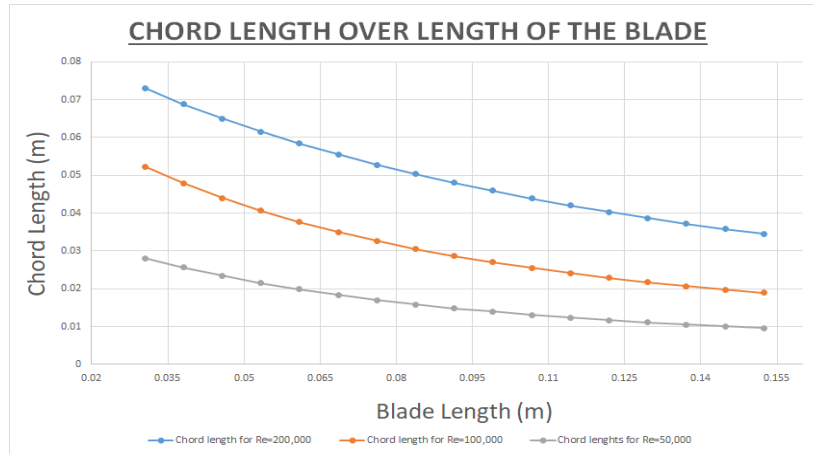
Figure 37: Change in Chord Length Along the Blade length at Different Reynold's No.

BLADE LENGTH SECTION	20%	25%	30%	35%	40%	45%	50%	55%	60%	65%	70%	75%	80%	85%	90%	95%	100%
CHORD LENGTH (m)	0.092036	0.084672	0.078344	0.072832	0.067983	0.06368	0.059837	0.056385	0.053271	0.050449	0.047882	0.04554	0.043396	0.041428	0.039616	0.037944	0.036397

Figure 38: Change in Blade Length's Chord length at 200,000 Reynold's No.

Reynold's Number:

Reynold's number is a crucial factor in the performance of an electric ducted fan as it directly influences the thrust and torque generated by the propeller. Reynold's number is a dimensionless quantity that measures the relative magnitude of the inertial forces to the viscous forces in a fluid, and it is used to determine the transition from laminar to turbulent flow. A higher Reynold's number indicates a higher level of turbulence in the fluid flow and can result in a reduction in the efficiency of the fan. On the other hand, a lower Reynold's number indicates a lower level of turbulence in the fluid flow and can increase the efficiency of the fan. For a Clark Y 11.7% smooth, Reynold's Number varies the relation of the angle of attack with the C_l / C_d ratio
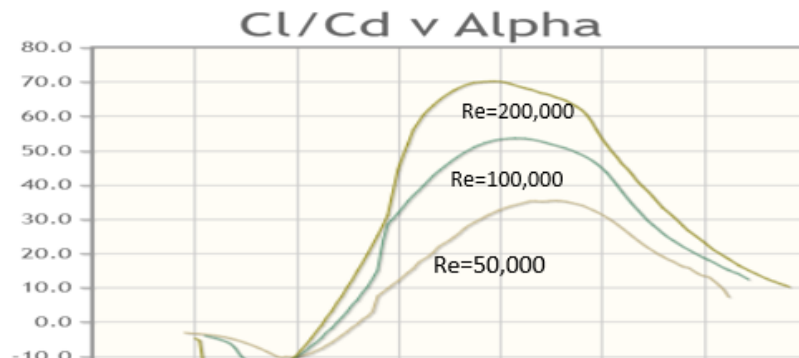
Figure 39: Relation of C_l / C_d with angle of attack at different Reynold's No.

From the table below, for a lower number of blades, the thrust requirement is provided by a higher Reynold's Number.

Table 2: Thrust Generated at the EDF with varying number of blades and Reynold's Number

No. of Blades	At Re=50000, Thrust (N)	At Re=100000, Thrust (N)	At Re=200000, Thrust (N)
1	1.88	3.76	7.53
2	3.76	7.52	15.06
3	5.64	11.28	22.59
4	7.52	15.04	30.12
5	9.4	18.8	37.65
6	11.28	22.56	45.18
7	13.16	26.32	52.71
8	15.04	30.08	60.24
9	16.92	33.84	67.77
10	18.8	37.6	75.3

Relation of Power, RPM, and Torque:

The power and torque provided at different values of RPM were calculated and from the provided data it was concluded that for the required thrust of 30N for a small UAV at cruise condition the Power requirement of 1373W was being fulfilled at 5000 RPM. At a higher or lower RPM, the thrust will change and will not meet our requirement.
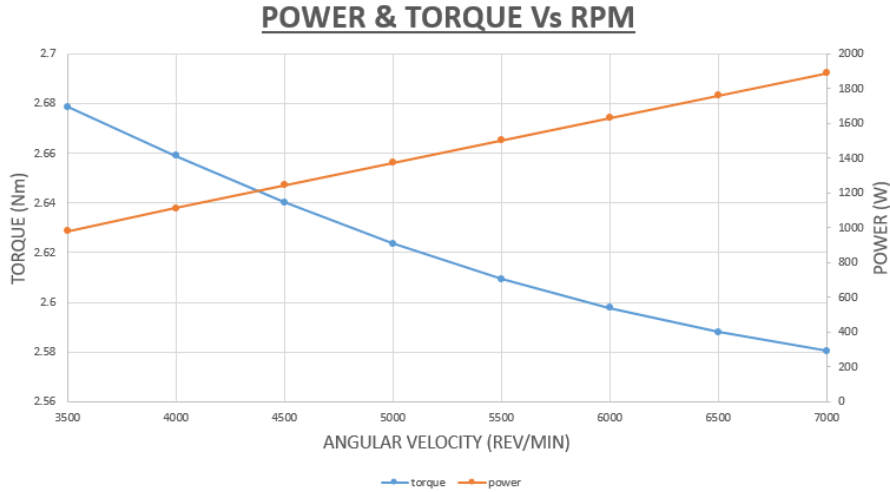
Figure 40: Power and Torque Vs RPM Graph

Number of Blades:

The number of blades on an electric ducted fan affects its thrust, power, and efficiency. More blades increase thrust and power but decrease efficiency due to increased drag. Fewer blades decrease thrust and power but increase efficiency by reducing drag. To optimize performance, factors like the diameter of the propeller, blade profile, and fluid flow conditions must be considered. Balancing the trade-off between thrust and power and efficiency is essential in selecting the number of blades. Hence the number of blades selected as per thrust requirement and optimum torque according to the lower power and higher efficiency is 4.
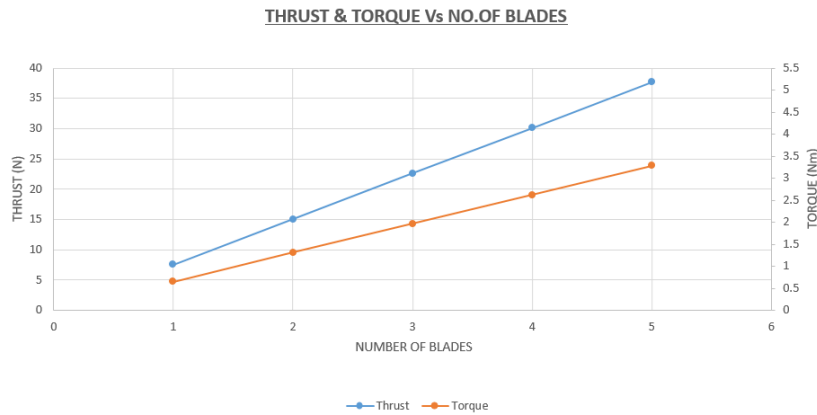
Figure 41: Thrust and Torque vs No. of Blades Graph

Power Required:

The power required by the EDF to generate the required thrust for our required cruise speed of 20 ms-1 are directly proportional. By increasing the requirement of cruise velocity we will need to increase hence increasing the size and weight of the battery. In order to keep it in a range of the required velocity, the power is calculated to be 1373W.
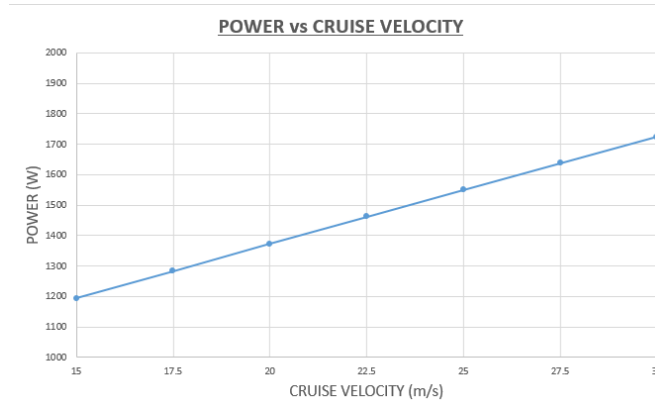

Figure 42: Power vs Cruise Velocity Graph

Duct Length:

The length of the duct in an EDF has a significant impact on its performance. A longer duct can improve pressure recovery, but also increases losses and reduces efficiency. In contrast, a shorter duct reduces pressure recovery and losses, but can increase efficiency. To optimize the duct length, factors such as flow rate, velocity, and pressure drop within the duct should be considered. Structural design must also be optimized to ensure that the fan can handle the additional load

Duct Shape:

The shape of the duct is a critical factor that can influence the performance of an EDF by affecting the flow rate, velocity, and pressure drop within the duct. A well-designed duct can improve performance by reducing losses and improving the flow into the fan. To optimize the duct shape, the aerodynamic design of the duct must be considered. The diffuser expansion ratio and airfoil-like shape of the walls are two factors that can be adjusted to optimize performance. Additionally, the structural design of the duct should be considered to ensure that it is structurally sound.

Duct Diameter:

The diameter of the duct is another important parameter that affects the performance of an EDF. A larger diameter duct provides higher pressure recovery and improved performance, but also increases the size and weight of the fan. Conversely, a smaller diameter duct reduces the size and weight of the fan, but also decreases pressure recovery and reduces

performance. The duct diameter ultimately depends on the desired output thrust and should be optimized accordingly.

Duct Clearance:

The duct clearance, which refers to the gap between the outer surface of the propeller blades and the inner surface of the duct, is a critical parameter that affects the performance of an EDF. A smaller duct clearance can improve performance by reducing losses and increasing pressure recovery, but also increases the risk of blade tip strikes and other mechanical failures. Conversely, a larger duct clearance reduces the risk of mechanical failures but also reduces performance. To optimize the duct clearance, both aerodynamic performance and mechanical safety must be considered. Manufacturing and assembly processes should also be considered to ensure ease of manufacturing and assembly.

Results from CFD analysis:

Once analytical calculations had been done and we had designed the propeller according to these calculations, the next step is to verify whether the propeller will create the required measured thrust when given the initial boundary conditions that we assumed when doing the calculations.

To perform simulation to measure the thrust produced by the propeller, ANSYS Fluent is used. Two domains were created around the propeller. The smaller domain is the one that rotates, and the bigger domain is stationary. We used k-epsilon conditions because the flow passing through the propeller becomes turbulent and turbulence in this condition is best described by k-epsilon condition.

The next step is to give the boundary conditions. The first boundary condition is that the propeller is attached to a bird moving with 20 m/s. To simulate this condition, we give the air entering the static domain a velocity of 20 m/s which is equivalent to prop moving with the same speed in opposite direction. The second boundary condition is the rotation of propeller. To simulate this, the rotary domain is rotated with 5000 rpm. The final required boundary condition is the pressure. The pressure in the static domain is set to atmospheric pressure.

After defining the boundary condition, the next step is to select a solver. For this simulation, CDAT for CFD-Post & EnSight was used. After initialization, we run the simulation and the thrust force came out to be **26.9 N**. The thrust force calculated analytically was 30.1 N. So the percentage error in our simulation reading is,

$$error = \frac{30.1 - 26.9}{30.1} \times 100 = 10.63\%$$

This much error is allowed in simulation which can be due to combination of many different reasons. The value of thrust force printed on the ANSYS console is shown in the following figure

```
Forces - Direction Vector (0 1 0)
                        Forces (n)
Zone                    Pressure         Viscous          Total
propeller               27.147992        -0.22710349      26.920889
----------------------- ---------------- ---------------- ----------------
Net                     27.147992        -0.22710349      26.920889
```

Figure 43: Ansys console: Force in y-direction (thrust-force)

After getting the desired results we see the pressure and air velocity distribution across the blades of propeller. The pressure profile shown in the figure below matches with the theory as the pressure above the blades is less than the pressure below. Maximum pressure is at the bottom side of the blades.
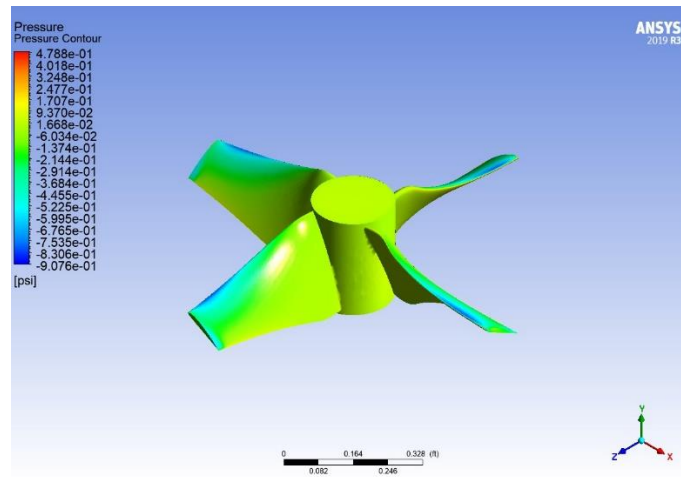
Figure 44: Pressure Contour

By our theoretical understanding we also know that velocity of air is maximum at the tip and is minimum near the hub. This is because as we move away from hub the radius of rotation increases and hence the tangential velocity also increases. This is also shown in the velocity contour of propeller.
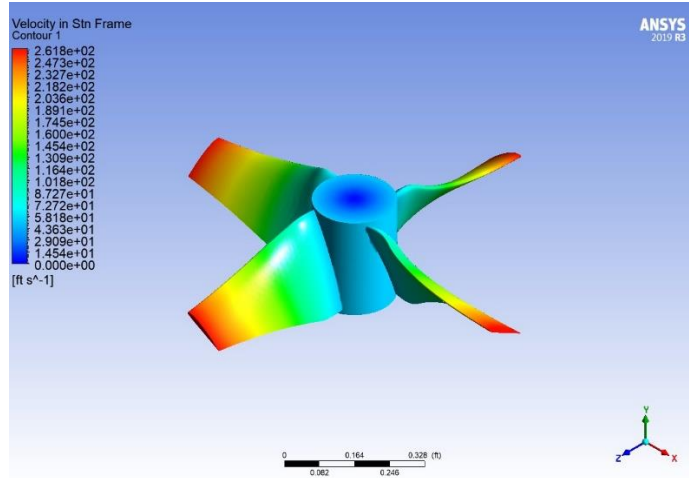
Figure 45: Velocity contour

Here you can see the maximum velocity is at the tip of blade and minimum at the hub.

Results from FEA analysis:

Once we had ratified our CFD results, and compared them with our analytical calculations, we needed to look at FEA results, based on the forces applied on the blade, and the stresses developed on the joints. We also needed to see the materials that were available to us, since we want to 3d print both the propeller, and the duct. For our material considerations, we looked at ABS and PLA, since both materials are locally available, used for 3d printing, and also provide considerable strength to be used in the project.

For both ABS and PLA, we can analyze the load cases, and relative displacements, as well as Von Moises stresses developed in the propeller. If we first look at ABS, this is what the total displacement under loading look like:
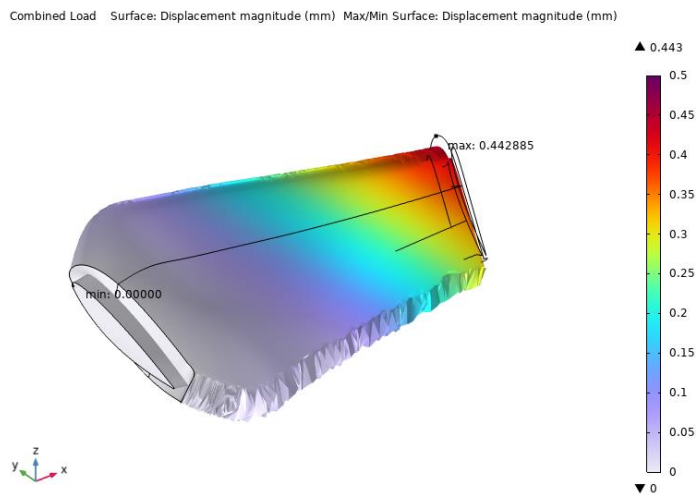
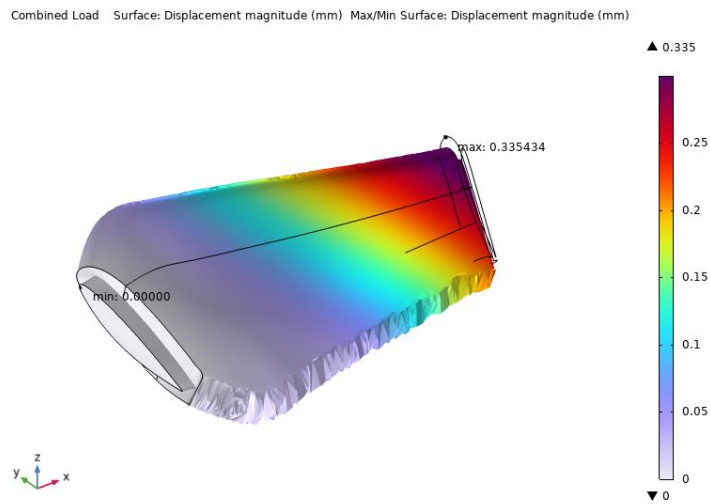**Figure 46:** **Displacement for ABS**
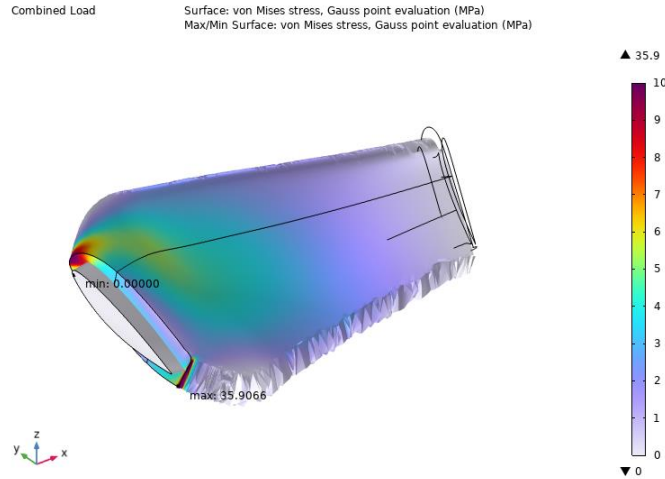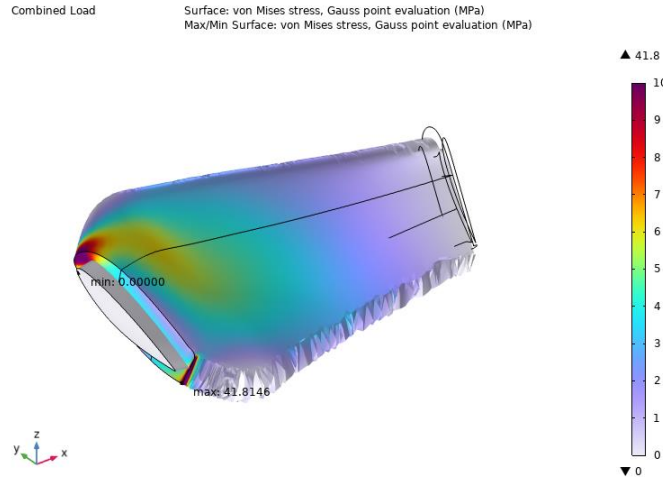
Figure 47*:* **Von Moises Stress for ABS**

Figure 48*:* **ABS Material properties**

In comparison to this, the following results were obtained for PLA:

Figure 49*:* **Overall displacement for PLA**

Figure 50*: Von Moises stress for PLA*

	Property	Variable	Value	Unit	Property grou
☑	Density	rho	1.24000000e+03	kg/m³	Basic
☑	Young's modulus	E	3.500[GPa]	Pa	Young's modu
☑	Poisson's ratio	nu	0.3	1	Young's modu

Figure 51*: Properties for PLA*

Now when we compare the results of our analysis, we find that PLA gives us a less critical value of net displacement, when compared to ABS. However Von Moises stress distribution, is more even for ABS as compared to PLA. Since we need to not only consider these two factors, but also structural integrity, costing, as well as other attributes like brittleness of materials. Keeping all of these factors in mind, we chose to go with ABS as our material for both the duct and propeller because:

1. ABS is less brittle than PLA, and will be able to withstand the high stresses developed once the fan starts moving.

2. For rapid prototyping, PLA is preferred, however, we want longevity in our prototype, which is why we will be preferring ABS over PLA in this regard.

Practical Design Considerations:

It is also important to note, that according to the relevant literature, not only will we have a loss of power within the drive train, but also we will also have a loss of power due to the propeller, depending on the efficiency of the propeller. As per *"General Aviation Aircraft Design"* by Snorri Gudmundsson, we can estimate both drivetrain losses and propeller efficiency based on the following figure:
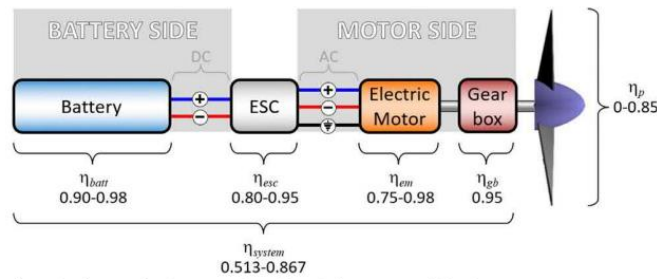
FIGURE 7-56 A schematic of a pure electric powertrain, with typical component efficiencies.

**Figure 52: Drivetrain losses and propeller efficiency**

According to this estimate, our propeller should have a maximum efficiency of 85%. Assuming an efficiency of 70%, that would give us a thrust value of 18.83 N. When we performed our testing with the open propeller, that gave us a value of thrust of about 1.6 kg, or 16 N. This gives us an error of 15%, which is acceptable. Furthermore, if we take into account the drivetrain losses, and compare it with the value of 18.83 N, we can also estimate that 15% of the power was lost Also to note: since our propeller was 3-D printed, there was bound to be a lesser efficiency value, which can be approved on based on the results and the change in material.

Figure 53: Open propeller testing

Then once we added the duct to the open propeller, the value of force then increased from 1.6 kg, to 2.1 kg, which is a 24% increase in the output thrust, which also further validates our results of the duct significantly improving thrust capability for our propeller. Once again, once the material considerations have been improved we can have a much greater value for thrust as well, and up to a 30-40% increase in thrust. Furthermore, we can also improve the thrust capability for our duct, by working on the optimization of the duct shape, and the inlet and exit angles, as well as the internal and external aerodynamics of our duct.
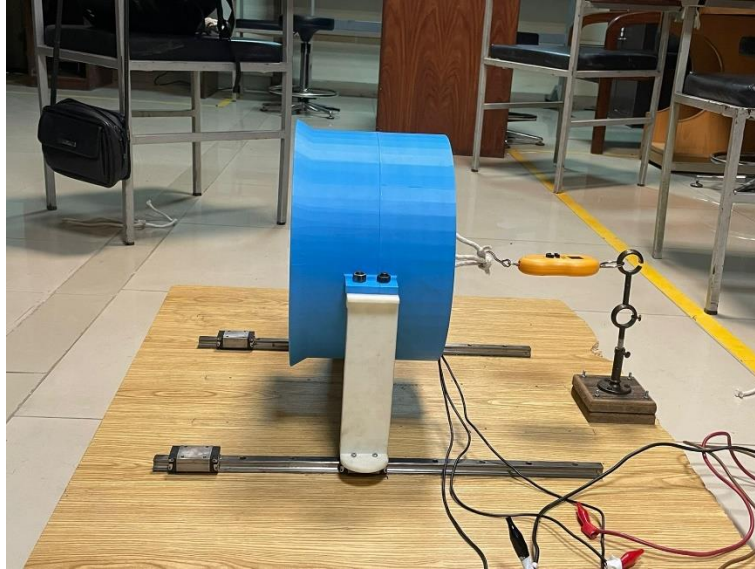
Figure 54: EDF testing

Testing and Results:

The following two tables look at the number of tests that we ran for both the open propeller, and the EDF (for comparison). In both cases, the value for static friction was also calculated, and then added to every value to apply for correction of the values:

Table 3: Force calculation for open propeller

Sr. No.	Force (kg)	Corrected Value (kg)
1	1.420	1.57
2	1.450	1.60
3	1.420	1.57
4	1.420	1.57
5	1.510	1.66
6	1.400	1.55
7	1.520	1.67
8	1.510	1.66
9	1.510	1.66
10	1.420	1.57

Value of Friction = 0.15 kg

Table 4: Force calculation for EDF

Sr. No.	Force (kg)	Corrected Value (kg)
1	1.710	2.03
2	1.710	2.03
3	1.710	2.03
4	1.710	2.03
5	1.710	2.03
6	1.920	2.24
7	1.920	2.24
8	1.920	2.24
9	1.920	2.24
10	1.920	2.24

Value of Friction = 0.32 kg

CHAPTER 5: CONCLUSION AND RECOMMENDATION

Conclusion:

This thesis project focused on the fabrication and optimization of a fan system according to concluded analytical results from Computational Fluid Dynamics (CFD) and Finite Element Analysis (FEA) was the focus of this thesis project. The aim was to design fan design that met specific thrust and size requirements, then optimize it further using expensive and unique machining procedures as per our requirement, budget and demand to reduce losses.

The optimization process began with theoretical calculations to determine the fan's design parameters. The resulting design was used to fabricate and test a 3D-printed propeller made of ABS material, considering strength and material considerations into account. The fabricated propeller performed successfully, albeit with a 15% error. Exploring alternative machining techniques and materials revealed additional optimization opportunities.

While the initial fan design was developed using 3D printed material, the choice was primarily motivated by its lightweight and low-cost nature, making it ideal for testing. However, the use of 3D printed material resulted in flexing losses, emphasizing the need for improvement. To address this limitation and improve performance, the project proposes fabricating the propeller and duct out of lightweight sheet metals using casting and molding techniques. This modification to materials and manufacturing processes is intended to reduce losses and increase overall efficiency.

The successful design iterations and attainment of desirable efficiencies provided important insights into thrust optimization. The addition of a duct around the fan system resulted in a significant increase in thrust, demonstrating the importance of duct implementation. However, the project discovered a decrease in net thrust as a result of the tension force along the mass spring balance system, which acted in the opposite direction of the fan's thrust.

In conclusion, this thesis project successfully fabricated and optimized a fan system using the finalized results of CFD and FEA analyses. Initial testing with a 3D printed propeller demonstrated acceptable efficiency but identified areas for further improvement. The proposed shift to lightweight sheet metal casting and molding offers a promising opportunity to improve overall performance. Furthermore, investigating alternative 3D printing materials such as PETG and PLA opens up new avenues for future research. Due to time constraints, the project's results were limited to testing with ABS propellers and a PLA duct.

The project did, however, identify limitations and challenges, such as losses caused by flexing of the 3D printed material. To address these issues, the project proposed using lightweight sheet metals as well as casting or molding techniques. More research is needed to investigate the duct's design and material optimization, as well as alternative 3D printing materials. By addressing these issues, researchers can improve the performance, efficiency, and usability of EDF systems in a variety of applications.

Overall, this project advances our understanding of EDF system optimization while also providing valuable insights for future research and development. Further research into the duct's design and material optimization is recommended to achieve higher thrust values and better performance.

Recommendations:

Implementations in Various Drone Applications:

Investigate the use of advanced materials with higher strength-to-weight ratios and better aerodynamic properties. Examine the use of composite materials, such as carbon fiber-reinforced polymers (CFRP), to reduce weight while improving structural integrity. To ensure optimal performance and durability, conduct extensive material characterization and testing.

Material Optimization:

Advanced Material Optimization: Exploration of advanced materials is critical for further improving the EDF design. To reduce flexure losses, optimal materials with lower weight and higher strength and integrity should be investigated. Although more expensive, materials such as carbon fiber polymers have the potential to significantly improve efficiency and performance. To ensure the selection of the most appropriate materials for EDF fabrication, extensive research should be conducted to understand the trade-offs between cost, performance, and durability.

Noise Reduction:

Adding a duct to an open propeller can increase thrust while also lowering noise levels. This is an excellent opportunity for additional research and development. Investigating methods to reduce acoustics in EDF systems would aid in the development of more efficient and quieter designs. To reduce noise levels generated by EDF systems, researchers should investigate the use of noise-cancelling technologies and sound-absorbing materials. This study could result in innovative and captivating designs in the field of EDF technology.

Computational Simulations and Optimization:

Using computational simulations, such as CFD analysis, to optimize the design of the EDF system can be extremely beneficial. To analysis and refine the duct shape, curvature, and inlet/outlet configurations, researchers should run detailed simulations. Designers can explore a wide range of design variations and assess their impact on performance parameters such as thrust, efficiency, and noise levels by leveraging computational tools. This will allow researchers to make informed design decisions and improve the EDF system's performance.

Collaboration and Knowledge Sharing:

As the field of EDF technology evolves, collaboration among academia, industry, and research institutions is essential. Collaboration and knowledge-sharing initiatives can promote innovation and accelerate progress in the field. Collaboration among researchers, engineers, and manufacturers will facilitate the exchange of ideas, expertise, and resources, resulting in advancements in EDF design and fabrication techniques.

In conclusion, the recommendations for EDF design include implementation in various drone applications, advanced material optimization, noise reduction, computational simulations, and stakeholder collaboration. By following these recommendations, Pakistani

researchers and engineers can help to advance EDF technology, improving efficiency, performance, and application possibilities in the robotics, aeronautics, and aerospace industries.

REFRENCES

[1] (Brushless Vs Brushed DC Motors: When and Why to Choose One Over the Other, n.d.). Retrieved from: https://www.monolithicpower.com/

[2] (Brushless Inrunner vs Outrunner motor?, n.d.). Retrieved from: https://www.radiocontrolinfo.com/brushless-inrunner-vs-outrunner-motor/

[3] Gudmundsson, S. (2022). *General Aviation Aircraft Design* (Second Edition, pp. 620 – 630). Butterworth-Heinemann.

[4] Gudmundsson, S. (2022). *General Aviation Aircraft Design* (Second Edition, pp. 646 – 656). Butterworth-Heinemann.

[5] Gudmundsson, S. (2022). *General Aviation Aircraft Design* (Second Edition, pp. 647). Butterworth-Heinemann.

[6] Moaad, Y. (2013). *Design and optimization of a ducted fan VTOL MAV controlled by Electric Ducted Fans.* DOI: 10.13009/EUCASS2019-108

[7] Kubica, J. (2017). *Electric ducted fan theory.*

[8] Sherlock, S. *Compressibility: Selection of propeller airfoil section.* (Prandtl-glauert rule).

[9] Gudmundsson, S. (2022). *General Aviation Aircraft Design* (Second Edition, pp. 643 – 645). Butterworth-Heinemann.

[10] Buyung Junaidi, M. Ardi Cahyono. *Conceptual Design of an Electrical Ducted Fan (EDF)*

[11] Muhammad Abid Ali (2022). Design and Development of Electric Ducted Fan for Small UAVs

[12] (Gartt motor). Retrieved from: https://www.smarthobby.pk/product-page/gartt-ml-5210-340kv-4600gram-4-6kg-thrust-brushless-motor